

# **Model-Free Data Detection for Wireless Communication Using Machine Learning**

Bakhtyear Fahim  
Master of Engineering  
Electronics Engineering



School of Engineering Macquarie University

November 8<sup>th</sup>, 2025

Supervisor: Dr. Hazer Inaltekin

## **ACKNOWLEDGMENTS**

I would like to acknowledge and sincerely thank my supervisor, Dr. Hazer Inaltekin, for his expert guidance and encouragement throughout this research. I also thank the School of Engineering at Macquarie University for providing the academic support and resources needed to complete this work.

I also thank my family for their constant support and belief in me. I also thank my friends for their moral support and helpful feedback during the project.

# **STATEMENT OF CANDIDATE**

I, Bakhtyear Fahim, declare that this report, submitted as part of the requirement for the award of Master of Engineering in the School of Engineering, Macquarie University, is entirely my own work unless otherwise referenced or acknowledged. This document has not been submitted for qualification or assessment at any academic institution.

Student's Name: Bakhtyear Fahim

Student ID: 48712434

Student's Signature: *Bakhtyear*

Date: 08-11-2025

# **STATEMENT OF USING GENERATIVE AI**

I, Bakhtyyear Fahim, acknowledge the use of artificial intelligence (AI) and editing tools in the research project and the writing of this thesis.

In this work:

- I used ChatGPT (GPT-5) to help me brainstorm possible chapter outlines and section headings.
- I used ChatGPT (GPT-5) to help me with finding relevant sources for my literature review.
- I used code examples generated by ChatGPT v4 (o4-mini-high) to prototype the decision-boundary plots (see Chapter 4).
- I used ChatGPT (GPT-5) to generate ideas about prospects of this thesis (Chapter 5).

I am aware of the limitations of these AI tools and ultimately, I am responsible for all the content, the research, and the development of ideas described in this document.

Signature: *Bakhtyyear*

Date: 08-11-2025

# ABSTRACT

This thesis extends the previous Thesis-A work on model-free data detection for wireless communication. The entire thesis applies machine learning for wireless signal detection. In Thesis-A, we trained a SoftMax classifier to detect BPSK, QPSK, and 16-QAM symbols under AWGN without explicit channel knowledge. The model learned decision boundaries and achieved near-ML accuracy at moderate SNR. In Thesis-B, we extend this work to fading channels and pilot-assisted detection. The study uses SoftMax regression and GMM-based clustering to detect M-QAM symbols without explicit channel models. We evaluate the system under AWGN and flat-fading channels. We fix the SNR and vary the number of symbols to study the trade-off between training overhead and detection accuracy. The results show near-ML accuracy at moderate SNR with efficient training cost. This confirms that simple learning-based detectors can operate reliably in practical wireless environments without full channel knowledge.

# Contents

<b>ACKNOWLEDGMENTS .....</b>	<b>i</b>
<b>STATEMENT OF CANDIDATE.....</b>	<b>ii</b>
<b>ABSTRACT.....</b>	<b>iv</b>
<b>Contents .....</b>	<b>v</b>
<b>List of Tables .....</b>	<b>vii</b>
<b>List of Figures.....</b>	<b>viii</b>
<b>1 Introduction.....</b>	<b>2</b>
1.1 Motivation.....	2
1.2 Background & Problem Statement .....	3
1.3 Objectives & Deliverables .....	4
1.4 Thesis Organization .....	4
<b>2 Literature Review &amp; Related Work.....</b>	<b>5</b>
2.1 Machine Learning Based Detection.....	5
2.2 SVM Based Detection .....	7
2.3 K-Nearest Neighbors (KNN) Based Detection.....	8
2.4 Low-Complexity Soft Detection .....	10
2.5 Maximum-Likelihood Detection .....	11
2.6 Deep Unfolding-Based Detection .....	12
2.9 Summary of Gaps and Contributions .....	17
<b>3 Background &amp; Methodology.....</b>	<b>21</b>
3.1 System Overview .....	21
3.2 Logistic regression.....	21
3.2 SoftMax Regression.....	22
3.3 Deep Learning (DL).....	23
3.4 Simulation Setup.....	23
3.5 Maximum-Likelihood Detection .....	25
<b>4 Results &amp; Discussion.....</b>	<b>26</b>
4.1 Modulation Detection Results (GMM).....	26
4.2 Analysis of SoftMax Regression under AWGN .....	30
4.3 Analysis of SoftMax Regression under Fading Channels .....	35
4.4 Symbol-Error Probability Analysis .....	38
4.5 Number of Training Symbols and Goodput Analysis .....	41
4.6 Channel-Invariant Performance Analysis .....	42
4.7 Comparative Performance and Discussion of Results .....	44
4.8 Chapter Summary .....	46

<b>5 Conclusions &amp; Future Work.....</b>	<b>47</b>
5.1 Conclusion .....	47
5.2 Practical Implementation .....	48
5.3 Limitations and Challenges .....	48
5.4 Future Research Directions.....	49
<b>Appendix.....</b>	<b>50</b>
<b>References.....</b>	<b>52</b>

# List of Tables

Table 1: Summary of Traditional Approaches .....	17
Table 2: Minimum Reliable SNR for Accurate GMM Modulation Detection .....	43
Table 3: Comparison of SoftMax and ML Accuracy at 15 dB SNR.....	44

# List of Figures

Figure 1 A flowchart representing a single layer of DetNet.....	5
Figure 2 CNN Architecture for Automatic modulation Detection.....	6
Figure 3 Measured Phase Mismatch under Different Equalization Methods.....	7
Figure 4 Schema of the proposed AMR using SVM + PSO approach.....	8
Figure 5: Transmitted and received images- traditional vs KNN.....	9
Figure 6 Illustration of the proposed detection in the case of 64-QAM.....	11
Figure 7 Bit error rate vs. SNR with fixed $\zeta$ : constant unknown channel .....	12
Figure 8 64-QAM Output Using Blind Equalization .....	13
Figure 9 Block diagram for GMM-based modulation classification .....	14
Figure 10 Experimental setup for deep learning-based modulation recognition .....	16
Figure 11 Block diagram of the proposed modulation and data detection system .....	21
Figure 12 Example of logistic regression decision making on Iris flower data set .....	22
Figure 13 Example of SoftMax regression decision region on Iris flower data set .....	22
Figure 14 Constellation diagram of 16-QAM simulation using python.....	24
Figure 15 Modulation Prediction for 32-QAM in Different SNR under Rician Channel .....	27
Figure 16 Incorrect Modulation Prediction in Low SNR Under Fading Channel.....	28
Figure 17 Modulation Prediction for 8-QAM for Different Channels at 10 dB SNR.....	28
Figure 18 Modulation Prediction for QPSK in Low SNR under Rician Channel.....	29
Figure 19 Repeated Modulation Detection Results under Fading Conditions .....	30
Figure 20 SoftMax Decision Boundaries for BPSK under AWGN .....	31
Figure 21 SoftMax Decision Boundaries for QPSK under AWGN .....	32
Figure 22 SoftMax Decision Boundaries for 16-QAM under AWGN .....	33
Figure 23 SoftMax Decision Boundaries under AWGN.....	34
Figure 24 SoftMax Decision Boundaries for 8-QAM under Fading.....	35
Figure 25 SoftMax Decision Boundaries for 16-QAM under Fading.....	36
Figure 26 SoftMax Decision Boundaries for 32-QAM under Fading.....	37
Figure 27 16-QAM Detection: Symbol Error Probability vs. SNR - AWGN .....	38
Figure 28 16-QAM Detection: Symbol Error Probability vs. SNR - Rayleigh.....	39
Figure 29 16-QAM Detection: Symbol Error Probability vs. SNR - Rician.....	40
Figure 30 Symbol Error Probability vs Training Symbols for 32-QAM .....	41
Figure 31 Average Goodput vs Training Symbols for 32-QAM.....	42
Figure 32 Channel Invariance Rayleigh $\leftrightarrow$ Rician generalization for 32-QAM .....	43
Figure 33 SoftMax Accuracy with ML Detector's Accuracy .....	45

# Chapter 1

## Introduction

Wireless systems carry data over the air. They use radio waves to send and receive information. Noise and channel fading can cause errors in the received signal. Machine learning can help improve signal detection. SoftMax regression can classify QAM symbols. Convolutional neural networks can estimate channel state. This thesis studies machine learning methods for wireless links. It applies SoftMax regression to BPSK and M-QAM classification. We evaluated our model under varying noise levels.

Wireless communication carries information by sending symbols over the air. Modern systems often use QAM (quadrature amplitude modulation) to encode data. In QAM, each symbol is represented by a point in a two-dimensional constellation (in-phase vs. quadrature). Noise and interference in the channel blur those points. Detecting the correct symbol under noise is essential for reliable data transmission.

Traditional detectors rely on explicit channel models. For example, maximum-likelihood rules assume known gain and noise statistics. As modulation orders increase (e.g., 32-QAM, 64-QAM), analytical detectors become more complex or require perfect channel knowledge. In fast-changing environments, maintaining accurate models is difficult. A model-free approach could learn decision rules directly from data without requiring a precise channel formula.

In Thesis-A, we studied model-free machine learning for symbol detection. We used SoftMax regression to detect BPSK, QPSK, and 16-QAM symbols under AWGN. The model learned decision boundaries without knowing the channel. It achieved near-ML accuracy at moderate SNR. That work showed that simple learning methods can replace analytical detectors in clean channels.

This thesis extends that work to realistic wireless channels. We focus on fading, pilot-assisted learning, and goodput analysis. The receiver uses pilot symbols to learn the channel. We train and test model-free detectors under fading conditions. We fix SNR and vary the number of training symbols to study accuracy and overhead. We also measure goodput loss due to training. Results show that learning remains effective with fading. The system achieves high accuracy with limited number of training symbols. This confirms that simple ML detectors can support practical wireless links with low complexity.

### 1.1 Motivation

Machine learning offers a way to build “model-free” detectors. A classifier can be trained on noisy I/Q samples to learn decision boundaries between constellation points. Logistic regression (SoftMax) is a simple multiclass method that naturally yields linear boundaries in

the I/Q plane. SoftMax regression can serve as a lightweight, data-driven alternative to maximum-likelihood detection. Using SoftMax regression for M-QAM detection has several advantages:

- It can automatically detect the modulation type by looking at received signal only.
- It does not need an explicit channel model during inference, only samples and labels.
- Training can adapt to different noise levels and modulation orders by generating appropriate data.
- Training can adapt to different type of fading scenarios.
- The learned decision boundaries are linear and easy to visualize for insight.

This thesis extends SoftMax-based detection beyond the AWGN study in Thesis-A. We apply the model to both AWGN and fading channels and generate noisy I/Q samples for BPSK, QPSK, and 16-QAM. We train multiclass logistic regression to classify each noisy sample. The SoftMax classifier is trained to detect symbols without explicit channel equations. We then compare the learned decision boundaries to the theoretical ML boundaries. We also study the effect of number of training symbols by fixing SNR and varying training overhead. This allows us to observe how learning performance changes with channel variation and number of training symbols. Finally, we measure symbol-error probability versus SNR for both SoftMax regression and the classical ML detector. The results confirm that a simple model-free detector can achieve high accuracy with limited training symbols while keeping the system lightweight.

## 1.2 Background & Problem Statement

Wireless links use M-QAM modulation because it efficiently packs multiple bits per symbol. Noise and fading cause constellation points to shift or overlap. The receiver must decide which ideal symbol each noisy point represents. Maximum-likelihood (ML) detection minimizes error probability if the channel model is exact. However:

- ML detection complexity grows with  $M$  (number of constellation points).
- ML requires precise channel knowledge and noise variance.
- Fading changes the signal strength over time, so fixed decision rules become unreliable.
- Channel variations require frequent re-estimation, which increases overhead and delay.
- In practice, the channel estimate may be imperfect or change rapidly.

These challenges motivate a data-driven detector that learns to classify noisy symbols without requiring the channel formula at runtime.

## 1.3 Objectives & Deliverables

A software platform with the following algorithms:

- A machine learning algorithm for data detection in AWGN channels.
- Another machine learning algorithm for data detection over fading channels.
- A deep learning algorithm improving the performance of basic machine learning techniques.
- A logistic regression algorithm for detecting BPSK signals over AWGN & fading channels with unknown symbol probabilities.
- A SoftMax regression algorithm for detecting M-QAM symbols over AWGN channels.
- Evaluate symbol-error probability vs. SNR for SoftMax regression and ML detection.
- A trade off analysis between training time and algorithm accuracy.

## 1.4 Thesis Organization

The remainder of this thesis is organized as follows:

- **Chapter 2** reviews prior work on ML-based and analytic QAM detection methods.
- **Chapter 3** describes the system model, AWGN data generation, and dataset details.
- **Chapter 4** presents the SoftMax regression design, training procedure, and decision-boundary plots. Compares symbol-error results for SoftMax regression versus ML detection across SNRs.
- **Chapter 5** concludes with summary, limitations, and suggestions for future work.

# Chapter 2

## Literature Review & Related Work

This chapter reviews previous work on detecting QAM symbols and related tasks in wireless systems. All methods use either machine learning or analytical detection rules. We also previewed different techniques to detect the modulation scheme. We discussed each approach and provided a summary table.

### 2.1 Machine Learning Based Detection

Deep neural networks can learn to detect QAM symbols in MIMO channels without explicit formulas. Samuel et al. [1] proposed *DetNet*. *DetNet* unfolds an iterative optimization algorithm into a neural network. It learns from simulated channel data and predicts transmitted symbols (Figure 1). Tests show *DetNet* matches near-optimal detection with less computation.

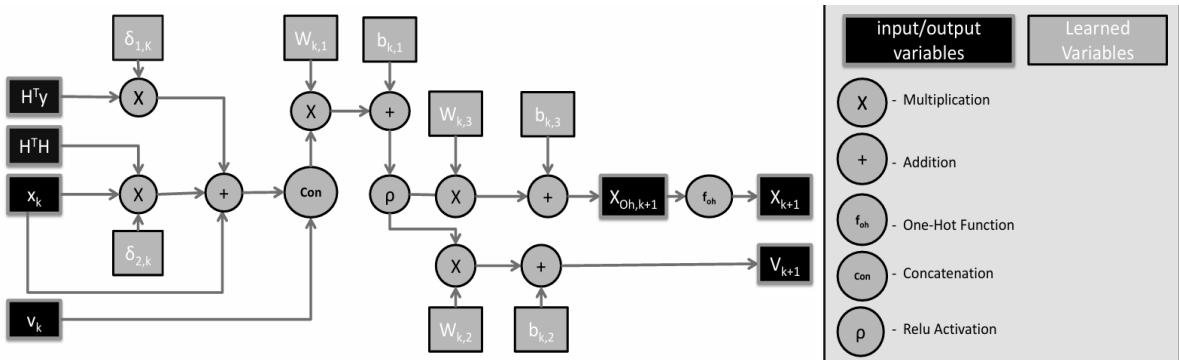
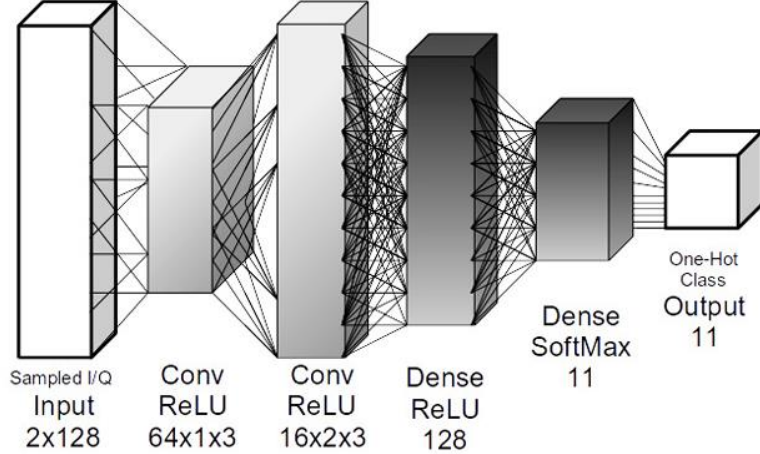


Figure 1 A flowchart representing a single layer of *DetNet* [1]

Samuel et al. [2] extended this idea in “Deep MIMO Detection.” They trained a network on many random channel realizations for various QAM orders. The model works well across changing channels. It outperforms classical message-passing by about 2 dB at a symbol-error rate of  $10^{-3}$ . However, both [1] and [2] need offline training for each channel type. They can be slow to retrain if channel statistics change. They presented an overview of both supervised and unsupervised learning approaches and categorized them into two main categories: likelihood-based methods and feature-based methods. These techniques are designed to classify the modulation schemes of incoming signals automatically.

Then N. Venkateswara Rao and B. T. Krishna [17] further explores the increasing role of machine learning models for AMR. Convolutional Neural Networks (CNNs), for example, are noted for their ability to automatically learn features directly from raw I/Q samples without needing manual feature extraction. Studies like O’Shea et al. [22] and Rajendran et al. [23] have

shown that CNNs can outperform traditional classifiers, achieving higher classification accuracy, especially at low SNRs. In addition to CNNs, the authors also mention the potential of Recurrent Neural Networks (RNNs), particularly Long Short-Term Memory (LSTM) networks, for handling temporal dependencies in signals, though they also require significant computational power and are more complex to train.



*Figure 2 CNN Architecture for Automatic modulation Detection [22].*

The architecture in Figure 2 represents the convolutional neural network (CNN) model proposed by O’Shea et al. [22], which is one of the earliest and most influential works applying deep learning to radio signal classification. The first convolutional layer has 64 filters of size  $1 \times 3$  and extracts local temporal patterns from the sampled I/Q data. The second convolutional layer uses 16 filters of size  $2 \times 3$  to capture higher-level spatial relationships between I and Q components. Each convolutional layer is followed by ReLU activation and dropout regularization to prevent overfitting. The dense layer with 128 neurons integrates the extracted features, and the final SoftMax layer with 11 outputs performs classification across modulation categories. The network receives raw in-phase (I) and quadrature (Q) samples as input and uses two convolutional layers followed by dense ReLU and SoftMax layers to classify modulation types.

The review [17] highlights that robustness is a significant challenge for AMR systems. Especially in multipath fading channels, channel variations, and imperfect channel knowledge. To address these issues, the authors mention the use of Gaussian Mixture Models (GMM), which have been applied successfully in previous studies, such as Dobre et al. [24] and Lin et al. [25], to improve modulation recognition in fading environments. GMM-based methods use a probabilistic model to represent the distribution of the received signal, allowing for better handling of channel distortions.

Another challenge discussed is the lack of large, publicly available datasets for training and testing AMR models. The authors argue that dataset scarcity and class imbalance are major obstacles, and they suggest synthetic data generation techniques such as Generative

Adversarial Networks (GANs) as a potential solution. These methods can help create more diverse and realistic datasets that better reflect real-world channel conditions.

These findings support the motivation of this thesis, which uses model-free learning techniques like SoftMax regression and GMM for modulation classification under fading channels. These models are lightweight, adaptable, and efficient, making them suitable for real-world wireless communication systems.

## 2.2 SVM Based Detection

In optical and RF links, hardware can add nonlinear distortion to QAM symbols. Weixer et al. [5] combined a Support Vector Machine (SVM) classifier with a nonlinear Volterra equalizer to correct these distortions in high-speed 16-QAM optical transmission. First, the Volterra equalizer reduces nonlinear interference. Then the SVM separates the 16-QAM constellation regions. Experiments on an 80 GBd dual-polarization link show a bit-error-rate (BER) improvement of about 1 dB over standard equalization. The method works well for optical fiber nonlinearity. But it is complex and not directly tested on RF AWGN channels. This resulted in a phase mismatch for their simulation.

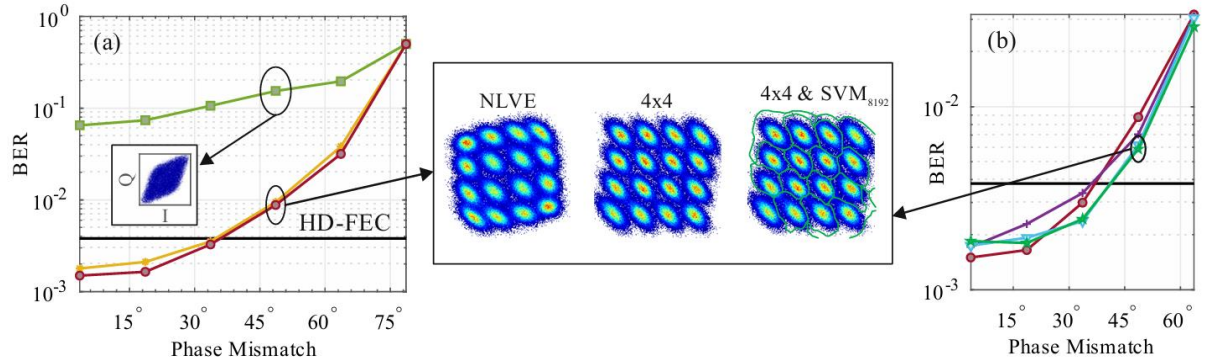
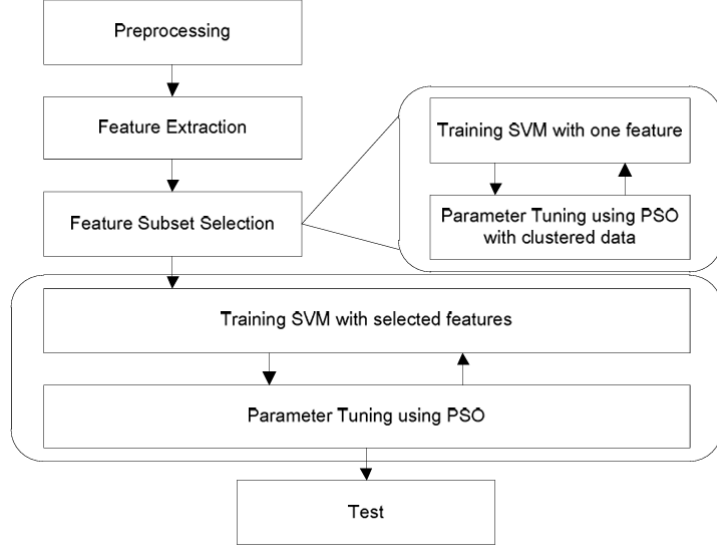


Figure 3 Measured Phase Mismatch under Different Equalization Methods [5].

Figure 2 shows: (left graph) Bit-error-rate (BER) plotted against increasing phase offset when only a single-stage equalizer is used (green curve), after applying a  $4 \times 4$  LMS MIMO equalizer (red), and with a nonlinear Volterra-type equalizer (NLVE, yellow). Insets show the constellation before and after equalization at a  $47.5^\circ$  phase error. (right curve) BER versus phase offset when using a  $4 \times 4$  LMS MIMO equalizer alone (red) and then following it with an SVM-based decoder trained on 2 048 (purple), 4 096 (blue), and 8 192 (dark green) pilot symbols.

In recent studies, Support Vector Machines (SVM) have been effectively applied to automatic modulation recognition (AMR) because of their strong classification capability in nonlinear environments. Valipour et al. [21] proposed an improved SVM-based framework combined with Particle Swarm Optimization (PSO) for parameter tuning and feature selection. Their method focuses on recognizing 16 different digital modulation types under additive white Gaussian noise (AWGN) conditions. The authors extract three categories of features from baseband signals: Spectral-based features, Statistical features, and Wavelet-based features. A total of 27 features are computed, and redundant ones are pruned using a PSO-based subset-

selection algorithm guided by classification accuracy. The proposed system adopts a hierarchical SVM structure.



*Figure 4 Schema of the proposed AMR using SVM + PSO approach [21]*

At the first layer, an inter-class SVM determines the modulation family (FSK, PSK, ASK, or QAM). At the second layer, multiple intra-class SVMs identify the exact modulation order within that family. PSO automatically tunes kernel parameters of each SVM to avoid manual trial-and-error. Simulation experiments were performed in MATLAB using generated PSK, ASK, FSK, and QAM signals over AWGN channels. Four SNR levels were tested: 6 dB, 9 dB, 16 dB, and infinite. The model achieved 96 % classification accuracy at 0 dB SNR, outperforming previous techniques by 1.5–3 %, and approaching 99.9 % accuracy at high SNRs. However, the method assumes that carrier synchronization is achieved and has not yet been validated for fading or time-varying channels.

Overall, these articles [5] and [21] support the integration of SVM-based classifiers with optimization algorithms for intelligent receivers in software-defined radio systems. It demonstrates that model-driven ML detectors can achieve high performance in noisy environments while remaining computationally efficient. It makes them suitable for inclusion in practical modulation-recognition pipelines.

## 2.3 K-Nearest Neighbors (KNN) Based Detection

The K-Nearest Neighbours (KNN) algorithm is a simple and non-parametric machine learning technique that classifies data based on proximity to labelled samples in a feature space. In modulation recognition, KNN works by comparing the received noisy signal features with a database of known modulation patterns and assigning the class of the nearest neighbours. It does not rely on prior knowledge of the channel model or statistical assumptions, which makes it suitable for adaptive wireless communication systems.

Sharanya Krishnamurthy et al. [6] presented a KNN-based symbol detector, for M-QAM systems to reduce bit-error rate (BER) under additive white Gaussian noise (AWGN) and phase noise. The study demonstrates that traditional QAM demodulation suffers significant distortion due to phase noise introduced by local oscillators in mmWave systems. The proposed method treats symbol detection as a classification problem in the I/Q domain, where each symbol corresponds to a class, and the Euclidean distance metric determines the closest match. Using MATLAB simulations and ADALM-Pluto software-defined radios (SDRs), the authors compared conventional demodulation with KNN detection for 64-QAM transmission. Results show a 4–6 dB improvement in BER when using KNN. The optimal performance was achieved at  $K = 5$  and 10 000 pilot samples. The study concludes that KNN provides a reliable and low-complexity solution for symbol detection in real-world channels affected by phase and amplitude noise. They claim that their KNN based architecture quantifies the received gain compared to the usual method. This method also keeps the phase noise constant.

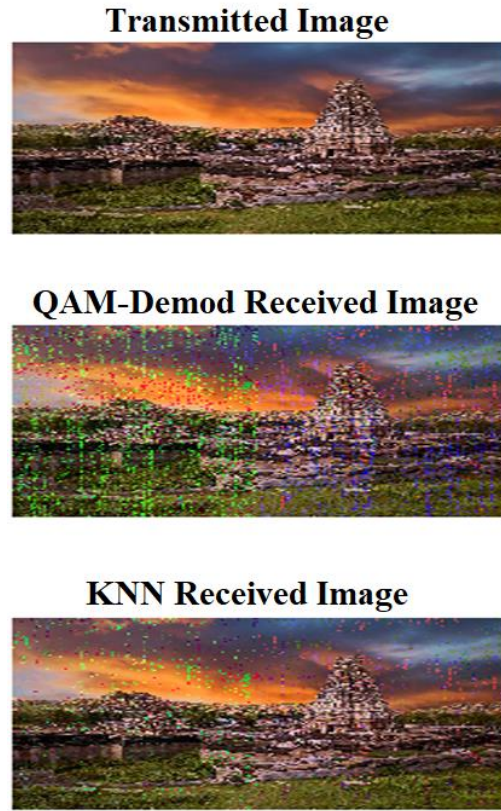


*Figure 5: Transmitted and received images- traditional vs KNN [6]*

The images in Figure 5 illustrate the comparative performance between traditional QAM demodulation and the proposed KNN-based detection method under phase noise conditions. The transmitted image represents the original data sent over the channel. The QAM-demodulated image shows severe distortion and pixel errors due to phase noise and nonlinear interference. In contrast, the KNN-reconstructed image retains most of the original color and structure, indicating improved symbol recovery and reduced bit errors.

A related study by Y. Alamri et al. [26] proposed a hybrid KNN–Genetic Programming (GP) approach for automatic modulation classification. Genetic programming is used to evolve feature-selection rules and optimize the KNN classifier parameters. The hybrid model improves both accuracy and generalization capability across noisy environments. Simulation results show that the GP-KNN model performs better than traditional KNN, especially at low SNR, where genetic optimization helps select discriminative features automatically rather than manually designing them. The study demonstrates that combining evolutionary computation with KNN can significantly enhance classification reliability in complex modulation recognition tasks.

M. Venkata Subbarao and P. Samundiswary [27] developed a KNN-based automatic modulation classifier (AMC) for adaptive radio systems. The classifier was trained on M-PSK and M-QAM signals under non-ideal channel conditions including multipath fading and AWGN. From a pool of 39 statistical features, 11 noise-robust features were selected using rough-set theory to minimize computation time. Six KNN variants were tested: Fine, Medium, Coarse, Cosine, Cubic, and Weighted KNN, each using different distance metrics. Experimental results across 0 – 20 dB SNR show that Cubic and Weighted KNNs achieved the highest accuracy, while Fine and Medium KNNs performed better for lower modulation orders. The authors highlight that KNN is computationally efficient, adaptable to fading conditions, and can achieve over 80 % classification accuracy at 0 dB SNR, confirming its suitability for real-time spectrum monitoring and electronic warfare systems.

KNN based models are independent from channel models and parameter estimation. KNN is a simple and data-driven method that can support low-complexity receiver design. However, it has some drawbacks. It depends heavily on the size and quality of the training dataset and becomes slower as the dataset grows. It also lacks adaptability in changing wireless environments unless retrained.

## 2.4 Low-Complexity Soft Detection

Soft-output detectors generate probability values that represent how confident the system is about each detected bit. These reliability values help improve performance during iterative decoding. Haroun *et al.* [7] proposed a low-complexity soft demapper for a  $2 \times 2$  MIMO system using QAM modulation. Their approach uses lattice reduction to simplify the channel matrix before performing detection.

The algorithm reduces the number of distance calculations required for soft-bit estimation, which lowers computational cost. Simulation results show that the method reduces complexity by up to 95% compared with standard belief-propagation demappers. Despite this reduction, the bit error rate (BER) performance remains close to the optimal Maximum Likelihood (ML) detector, within approximately 0.2 dB difference. However, this method was only evaluated on small-scale MIMO setups ( $2 \times 2$ ) and modulation orders up to 64-QAM. The performance for larger antenna systems or higher-order modulations has not been studied yet.

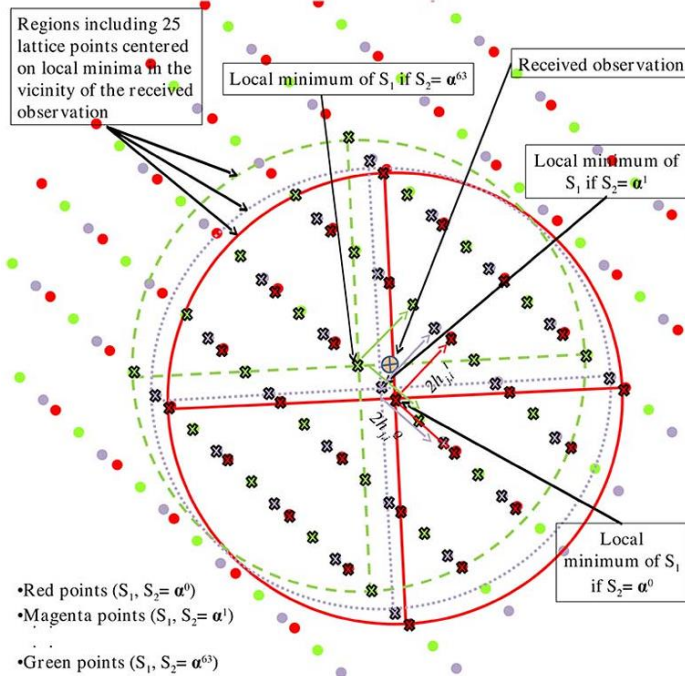


Figure 6 Illustration of the proposed detection in the case of 64-QAM [7]

Figure 6 illustrates the detection process for a 64-QAM constellation as described in [7]. The diagram shows the arrangement of constellation points and the corresponding local minima that represent possible detected symbols. Each color denotes a different symbol set, while the circles mark the decision regions used for detection. The figure highlights how the algorithm identifies nearby lattice points to reduce unnecessary computations. This visualization explains how the proposed method achieves low complexity while keeping detection accuracy close to that of ML performance.

## 2.5 Maximum-Likelihood Detection

Exact ML detection requires searching over all constellation points. Yoon et al. [9] derived a closed-form ML rule for square QAM in AWGN with a known channel gain. The rule computes a simple threshold test on real and imaginary parts. Complexity is  $O(M)$  instead of  $O(M^2)$  for brute-force search. Yoon provides exact SER formulas. The method achieves true ML performance with linear complexity in  $M$ . Its limitation is that it assumes a perfect channel estimate. It also applies only to single-antenna AWGN cases, not to MIMO or fading channels.

In practice, the channel is not known exactly. Xiao et al. [11] studied ML detection when channel estimates have error. He derives modified ML decision rules that incorporate a known channel error variance. For 16-QAM and 64-QAM, he shows an uncoded SER loss of about 2 dB versus perfect-CSI ML. With turbo coding, he further shows a coding gain of 0.5–1 dB. The drawback is that gains are marginal when channel error is small. Also, it assumes knowledge of error variance and still uses a lookup over all symbols.

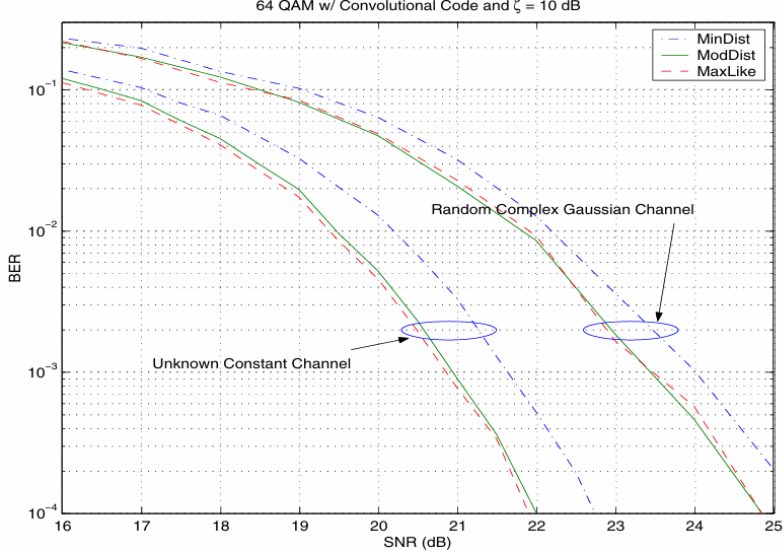


Figure 7 Bit error rate vs. SNR with fixed  $\zeta$ : constant unknown channel [11]

Figure 7 presents the bit error rate (BER) performance for 64-QAM under different channel conditions at a fixed  $\zeta = 10$  dB. Three detection methods are compared: Minimum-Distance (MinDist), Modified-Distance (ModDist), and Maximum-Likelihood (MaxLike). The results show that the MaxLike detector consistently achieves the lowest BER, confirming its optimality.

In the unknown constant channel, both ModDist and MaxLike detectors perform closely, with only a small gap between their BER curves. This indicates that the modified metric effectively compensates for channel uncertainty. However, when the channel varies randomly (complex Gaussian fading), performance degrades for all detectors. The MinDist method shows the largest BER, while the MaxLike method still provides noticeable improvement.

Xiao et al. [11] demonstrates that, incorporating channel uncertainty into the detection rule improves reliability, compared with simple distance-based detection. The modified and maximum-likelihood methods maintain strong performance even when the channel is not perfectly known. This confirms that probabilistic channel modeling can reduce detection loss in practical wireless environments.

## 2.6 Deep Unfolding-Based Detection

High-order QAM in OFDM can suffer from inter-symbol interference when the cyclic prefix (CP) is too short. Cai et al. [12] proposed DNN-IG, a deep neural network that unfolds an iterative grouping algorithm (ML-IG) for detection in OFDM with insufficient CP. Their DNN takes received I/Q samples, applies learned linear layers, and iteratively refines symbol estimates. For 256-QAM OFDM with a short CP, DNN-IG reduces BER by more than 1 dB compared to conventional iterative methods at 20 dB SNR. However, training is costly and specific to each CP length. Retraining is needed for different channel delays or CP designs.

If neither channel nor modulation order is known, blind methods are needed. Rao et al. [13] proposed a two-step blind method. First, they apply a simplified equalizer based on 4-QAM statistics to flatten the channel. Then they use a mapping function on the equalized I/Q samples

to detect the actual QAM order (4, 8, 16, 32, 64). Simulations show they achieve correct order detection down to 12 dB SNR with fast convergence. However, [13] does not provide detailed symbol-level error rates. It also assumes multipath channel effects can be handled by their 4-QAM equalizer, which may not hold in severe fading.

Often, the first step is to identify modulation type before detection. Ghodeswar and Poonacha [15] introduced an SNR-based adaptive classifier. They estimate SNR from received samples, then apply a hierarchical decision tree based on higher-order statistical cumulants. The method recognizes BPSK, QPSK, 8-PSK, 16-QAM, 32-QAM, and 64-QAM. At  $\text{SNR} \geq 10$  dB, they achieve over 95 % classification accuracy. Below 10 dB, accuracy degrades. This work focuses on modulation recognition rather than symbol detection. It also assumes AWGN and may fail under severe fading.

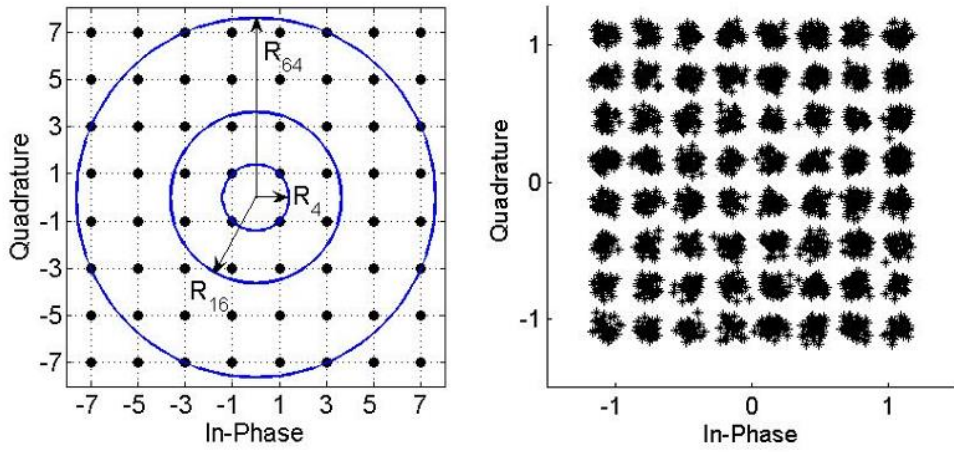


Figure 8 64-QAM Output Using Blind Equalization [13]

Figure 8 shows the 64-QAM output constellation obtained using the proposed blind equalization and order detection algorithm. In the left plot, the original 64-QAM constellation is displayed, where concentric circles  $R_4$ ,  $R_{16}$ , and  $R_{64}$  represent symbol clusters of different amplitude levels. These rings illustrate the hierarchical structure of the QAM modulation, with each circle corresponding to a different power region. The right plot shows the recovered constellation after blind equalization. Despite channel distortion and noise, the received points are correctly aligned with the 64-QAM grid. The clusters are well-defined and evenly spaced. It confirms that the algorithm effectively compensates for intersymbol interference and channel distortion without using training sequences. This result demonstrates that the proposed method can accurately equalize and identify higher-order QAM signals such as 64-QAM by exploiting the coordinate relationships of lower-order constellations like 4-QAM.

Often, the first step is to identify modulation type before detection. Ghodeswar and Poonacha [15] introduced an SNR-based adaptive classifier. They estimate SNR from received samples, then apply a hierarchical decision tree based on higher-order statistical cumulants. The method recognizes BPSK, QPSK, 8-PSK, 16-QAM, 32-QAM, and 64-QAM. At  $\text{SNR} \geq 10$  dB, they achieve over 95 % classification accuracy. Below 10 dB, accuracy degrades. This work focuses on modulation recognition rather than symbol detection. It also assumes AWGN and may fail under severe fading.

## 2.7 GMM Based Modulation Classification

As Liu et al. proposed a modulation classification approach based on Gaussian Mixture Models (GMM) for digital signals transmitted through multipath fading channels [16]. The aim was to identify modulation schemes such as ASK, FSK, PSK, and QAM under realistic wireless conditions that include both noise and fading. Traditional decision-theoretic detectors like Maximum Likelihood (ML) achieve optimal results when channel parameters are perfectly known, but their complexity and sensitivity to model mismatch make them impractical for time-varying channels. Similarly, conventional pattern recognition techniques based on higher-order statistics or cyclic cumulants are computationally heavy and less effective at low SNRs.

The proposed GMM method models the received signal's amplitude and phase distribution using a weighted sum of Gaussian components. Each modulation type is represented by a set of GMM parameters—means, covariances, and weights—stored in an offline database. The Expectation-Maximization (EM) algorithm is applied to estimate these parameters. To classify an incoming signal, the Kullback–Leibler (K–L) divergence is used to measure the dissimilarity between the received signal's GMM and the reference GMMs in the database. The modulation type with the smallest K–L distance is selected as the detected scheme.

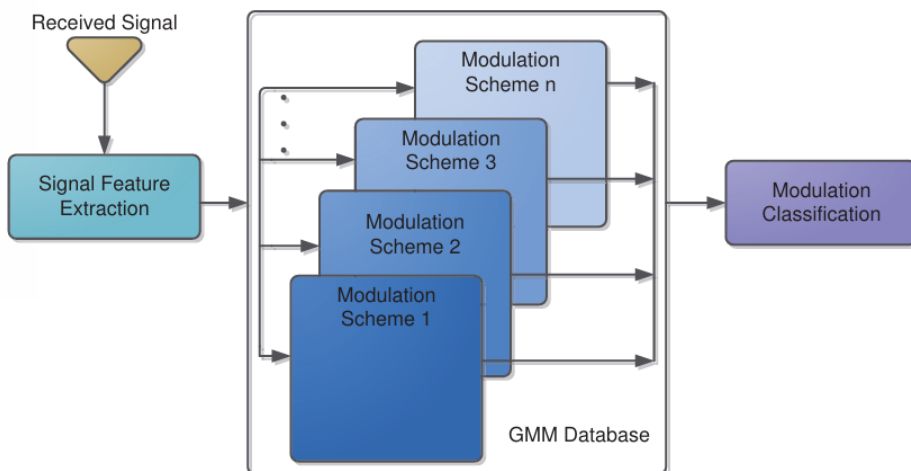


Figure 9 Block diagram for GMM-based modulation classification [16]

To address fading effects, the authors introduced an iterative Maximum A Posteriori (MAP) channel estimation process that refines the multipath coefficients and mitigates channel distortion before classification. This iterative structure effectively combines statistical channel estimation with probabilistic signal modeling. In each iteration, the estimated channel is updated, the received signal is compensated, and the GMM parameters are recalculated. The process continues until convergence, or a fixed iteration count is reached.

Monte Carlo simulations were performed for several modulation types including 2ASK, 2FSK, BPSK, QPSK, 16QAM, and 64QAM under AWGN and Rayleigh fading. The results showed that the proposed GMM classifier achieved significantly higher correct classification probability ( $P_{cc}$ ) than both ML-based and higher-order statistics (HOS) based methods,

particularly at low SNRs and under multipath fading conditions. The iterative MAP process improved accuracy with each iteration and successfully reduced multipath interference.

This work [16] demonstrates that a GMM-based model can represent the statistical distribution of modulated signals more flexibly than analytic models. It provides robustness against channel variation and model mismatch while maintaining moderate computational cost through Gaussian approximation. The integration of EM, MAP, and K–L divergence forms a complete framework that bridges traditional signal processing and probabilistic learning methods for wireless modulation recognition.

## 2.8 Deep Learning Based Modulation Classification

Recent literature shows that deep learning (DL) has become the dominant approach for automatic modulation classification (AMC) due to its ability to extract complex features directly from raw signal data. Several studies [18], [19], and [20] present a comprehensive overview of this transition from traditional feature-based methods to data-driven neural architectures.

Naveen et al. [18] compares classical machine learning methods (SVM, KNN, Random Forest) with deep learning models for modulation classification in their article *Classification of Automatic Modulations using Deep Learning and Machine Learning*. The authors report that CNN-based models outperform conventional ML in noisy and fading channels because they automatically learn hierarchical features from I/Q data. The study highlights that deep architectures can generalize across multiple modulation types such as BPSK, QPSK, 8PSK, and 16QAM. The authors also note that combining convolutional layers with recurrent structures (e.g., CNN-LSTM) improves temporal feature capture, achieving higher classification accuracy at low SNR. However, they emphasize that training deep models requires large datasets and computational resources, which can limit real-time deployment.

A deep learning for modulation recognition survey by Zhou et al. [19] reviews deep learning methods for AMC and provides experimental demonstrations under real wireless environments. It discusses the application of CNNs, RNNs, LSTMs, and hybrid architectures like CLDNN (Convolutional, Long Short-Term Memory, Deep Neural Networks). The authors analyze architectures such as ResNet and DenseNet, showing how deeper layers improve feature extraction in complex fading channels. The demonstration confirms that CNNs can maintain over 90% accuracy for SNRs above 5 dB, while traditional ML models degrade rapidly under the same conditions. The study also stresses the need for transfer learning and model compression to enable DL deployment in embedded wireless systems.

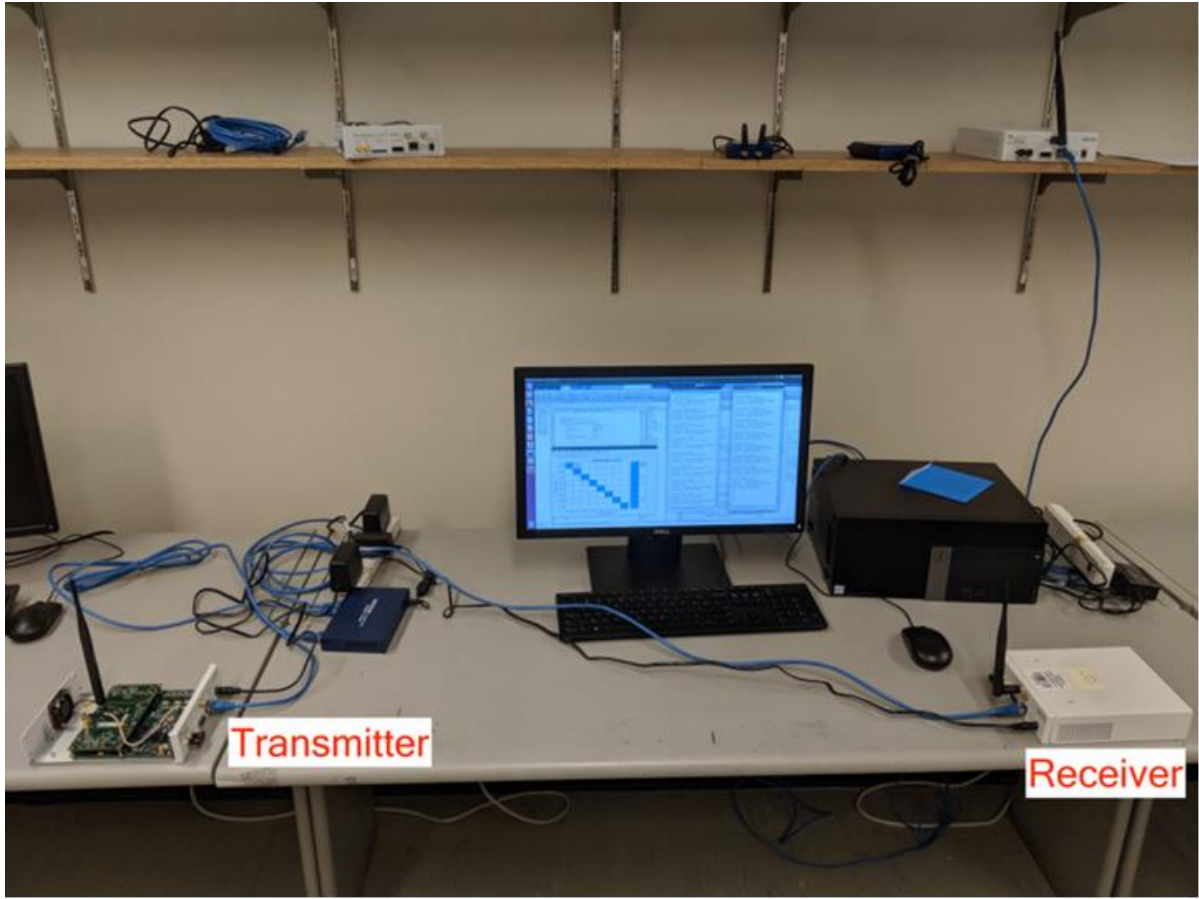


Figure 10 Experimental setup for deep learning-based modulation recognition [19]

The setup shown in Figure 10 illustrates the real-world testbed used in the study by Zhou et al. [19] *Deep Learning for Modulation Recognition: A Survey with a Demonstration*. The system consists of a transmitter and receiver connected through wireless channels. The transmitter sends modulated signals, while the receiver collects data for training and testing deep learning models. The computer in the middle controls the transmission process, captures received signal samples. The computer also processes them for analysis using frameworks such as TensorFlow and Keras. This experimental configuration validates the performance of convolutional and recurrent neural networks for automatic modulation recognition under real channel conditions, demonstrating the practicality of deep learning-based detection beyond simulation environments.

The study by Ghunaim et al. [20] classifies deep learning-based AMC techniques into three categories: feature-based (FB-AMC), blind recognition (BR-AMC), and likelihood-ratio test (LRT-AMC). CNNs are identified as the most frequently used models (24 papers), followed by LSTM, DNN, and RNN architectures. The survey finds that 65% of studies used feature-based AMC, while blind recognition approaches gained traction after 2016 with the introduction of end-to-end learning. It also examines performance metrics—accuracy, F1-score, recall, and confusion matrix. It notes that most papers rely on the *RadioML 2016.10a dataset*. The authors report that supervised and semi-supervised learning dominate AMC research, accounting for nearly 65% of implementations. TensorFlow and Keras are the most common

frameworks, used in 71% of surveyed studies. The paper concludes that CNN-based architectures consistently outperform others, providing robustness in low-SNR and fading conditions, while future work should focus on lightweight models for real-time signal recognition.

Together, these studies confirm that deep learning-based AMC systems can outperform both traditional and shallow ML models in accuracy and generalization. CNNs and hybrid networks (CNN-LSTM, CLDNN) dominate due to their capacity to learn both spatial and temporal patterns from I/Q data. However, challenges remain regarding data requirements, model interpretability, and computational efficiency. These findings strongly justify the continued exploration of model-free, data-driven approaches such as those implemented in this thesis for reliable wireless symbol detection.

## 2.9 Summary of Gaps and Contributions

The literature review shows that deep learning models perform well for symbol and modulation detection. CNN and hybrid networks such as CNN-LSTM or CLDNN achieve high accuracy in fading channels [18], [19], [20]. They can automatically learn spatial and temporal features from I/Q data. However, they need large datasets, long training time, and high computational power. These factors make them difficult to use in real-time systems.

Classical machine learning methods such as SVM [21] and KNN [6], [26], [27] are simpler and less computationally expensive. They work well for special cases such as nonlinear or phase-noise-affected channels. However, they depend on feature extraction, have limited scalability, and perform poorly when the channel varies. They also need retraining when signal conditions change.

Analytical and closed-form detectors such as maximum-likelihood (ML) [7], [9] give the highest theoretical accuracy. They assume perfect channel knowledge, which is not practical in fast or unpredictable wireless conditions. Blind and hierarchical classifiers [13], [15] can detect modulation order without training data. However, they cannot perform symbol-level detection and are not suitable for dynamic fading.

The following research gaps are found:

1. Most systems rely on accurate channel estimation and fail when the channel model is unknown.
2. Deep learning methods provide good accuracy but need high computation and retraining.
3. Classical ML methods like SVM and KNN are less adaptive and have scalability issues.
4. Analytical detectors are model-dependent, and blind classifiers ignore symbol-level accuracy.

This thesis addresses these gaps through a SoftMax regression-based model-free detector for M-QAM symbols. The method does not need channel estimation and learns directly from noisy data. The main contributions are:

- Development of a lightweight SoftMax regression detector for M-QAM under AWGN and fading.
- Comparison of SoftMax with analytical ML and traditional ML detectors.
- Performance analysis under fixed SNR with varying training sizes to show trade-offs between accuracy and training cost.
- Validation that SoftMax achieves near-ML accuracy for BPSK, QPSK, and 16-QAM.
- Use Gaussian Mixture Models (GMM) to improve symbol clustering and robustness under fading.
- Provide a simple, adaptive, and efficient solution for real-time wireless communication systems.

Table 1: Summary of Traditional Approaches

Ref. No.	Methods	Performance / Result	Limitations
[1]	DetNet: deep neural network unfolding projected gradient descent for MIMO detection	Achieves near-optimal MIMO symbol accuracy with low runtime complexity; robust across multiple channel realizations	Requires offline training for each channel distribution; not proven for very large constellations
[2]	Deep MIMO Detection: neural network architecture trained on varying channel realizations	Outperforms AMP and SDR by $\sim 2$ dB at $10^{-3}$ SER; maintains high accuracy with significantly lower complexity	Needs retraining if channel statistics change significantly; neural net size grows with system dimensions
[5]	SVM-based detection combined with nonlinear Volterra equalizer for 80 GBd DP-16-QAM	Demonstrates BER improvement and IQ-imbalance tolerance up to $43^\circ$ phase mismatch	Focused on optical fiber nonlinearity; high Volterra filter complexity; not directly applicable to RF AWGN channels
[6]	K-Nearest Neighbors classifier for QAM symbol detection under phase noise	Reduces BER by $\sim 4\text{--}6$ dB compared to conventional detection at moderate SNR in phase noise	KNN lookup cost scales with training set size; limited evaluation to moderate QAM orders and phase-noise models
[7]	Conditioned detection with lattice-reduction for soft QAM demapper in $2\times 2$	Cuts Euclidean distance computations by $\sim 95\%$ with no performance loss vs. conventional BP soft	Tested only on $2\times 2$ MIMO; performance on larger antenna arrays or higher-order constellations not

	MIMO systems	detection	evaluated
[9]	Closed-form maximum-likelihood detection for square QAM	Achieves exact ML performance with $O(M)$ operations; complexity much lower than brute-force ML	Complexity still grows linearly with $M$ ; assumes precise channel estimate; limited to single-antenna systems
[11]	MaxLike and Modified MinDist detectors accounting for channel estimation error	Slight uncoded SER improvement; with turbo coding gains of 0.5–1 dB in 16-QAM and 64-QAM	Marginal uncoded gains only; requires knowledge of channel error variance; increased computational cost for metrics
[12]	DNN-IG: deep unfolding of ML-IG iterative grouping detection for high-order QAM OFDM	Outperforms ISIC by >1 dB in BER for 256-QAM OFDM with insufficient CP; robust to channel model mismatch	High DNN complexity for training; specific to OFDM with short CP; retraining needed for different CP lengths
[13]	Blind equalization + order detection via coordinate mapping using 4-QAM statistics	Equalizes higher-order QAM (4, 8, 16, 32, 64) and correctly detects order in simulation; fast convergence	Relies on known 4-QAM statistics; not a symbol-by-symbol detector; performance in multipath/fading not studied
[15]	SNR estimation + hierarchical classification using higher-order cumulants	Achieves >95 % modulation type recognition (16-, 32-, 64-QAM, BPSK, QPSK, 8PSK) at $\text{SNR} \geq 10$ dB; robust false-alarm rates	Focused on modulation classification, not detection; assumes accurate SNR estimate; performance degrades below 10 dB
[16]	GMM-based modulation recognition under multipath fading	Improved classification accuracy under Rayleigh fading using EM and MAP iterations	Limited to simulated data; higher computational load from iterative MAP
[17]	ML-based AMR review	Summarized ML classifiers (SVM, ANN, CNN) for modulation classification	Lacks hardware validation; limited analysis of fading channels
[18]	CNN and ML comparison for AMC	CNN outperforms SVM and KNN by 5–10% at low SNR; strong noise robustness	Requires large training dataset; high training time
[19]	DL survey with real SDR demonstration	CNN achieves >90% accuracy at $\text{SNR} > 5$ dB; validated on real hardware	High computation cost; needs model compression for deployment
[20]	Systematic review of DL techniques for	47 papers reviewed; CNN most frequent; accuracy	Few studies address low-SNR or real-time adaptation

	AMC	>95% for high SNR	
[21]	SVM + PSO modulation recognition	99.9% accuracy at high SNR; reduced feature redundancy	Assumes perfect synchronization; not tested under fading
[26]	GP + KNN hybrid classifier	Enhanced low-SNR classification via automatic feature selection	Genetic optimization increases runtime complexity
[27]	KNN for adaptive radio AMC	80% accuracy at 0 dB SNR; effective in multipath and AWGN	Sensitive to dataset scaling; distance metric affects accuracy

Our thesis builds on these studies by combining model-free symbol detection and modulation classification using data-driven methods. We first use a Gaussian Mixture Model (GMM) for automatic modulation detection. The GMM classifier estimates the probability distribution of I/Q data and identifies the modulation type from mixtures of Gaussian clusters. It works without prior channel information and performs well under fading conditions. This combined framework provides both symbol-level and modulation-level detection in a unified model-free system, achieving a balance between simplicity, adaptability, and accuracy.

In the second part, we use a SoftMax regression algorithm for symbol detection. The algorithm is trained on noisy I/Q samples for M-QAM under both AWGN and fading channels. It learns to classify received symbols without using any explicit channel equation. The detected decision boundaries are compared with the analytical Maximum Likelihood (ML) detector to measure accuracy and reliability. This method maintains the simplicity of logistic regression and can adapt to different QAM orders.

# Chapter 3

## Background & Methodology

This chapter presents the theoretical foundations and practical steps used in this thesis. We first review key machine-learning methods: logistic regression, SoftMax regression, support vector machines (SVM), and deep learning (DL). We then describe the development of the simulation setup, and the maximum-likelihood (ML) detection rule.

### 3.1 System Overview



Figure 11 Block diagram of the proposed modulation and data detection system

Figure 11 shows the overall block diagram of the proposed modulation and data detection system. The system receives an input signal with unknown data and modulation scheme. The first block detects the modulation type using the Gaussian Mixture Model (GMM) classifier. Once the modulation scheme is identified, the signal is passed to the second block, where the SoftMax regression-based detector performs data detection. The detected symbols are then mapped to the corresponding output data. This two-stage structure enables both modulation recognition and symbol detection without using explicit channel models.

### 3.2 Logistic regression

Logistic regression is a statistical method for binary classification. It models the probability that a given input belongs to one of two classes. The model computes a weighted sum of input features and passes it through a sigmoid function. Training minimizes the cross-entropy loss using gradient descent. Logistic regression is simple, fast, and interpretable, but it handles only two classes. The sigmoid function for logistic regression is defined as:  $f(x) = \frac{1}{1+e^{-x}}$ .

Figure 12 shows how logistic regression performs binary classification using the Iris flower dataset. The model separates two classes: *Setosa* and *Not-Setosa*, based on sepal length. The red curve represents the logistic prediction function, which maps the input feature to the probability of belonging to the *Not-Setosa* class. Points below the curve are classified as *Setosa*, and points above are *Not-Setosa*. This example demonstrates how logistic regression converts continuous input values into class probabilities using a sigmoid function, forming the basis for

multi-class SoftMax regression used later in this thesis.

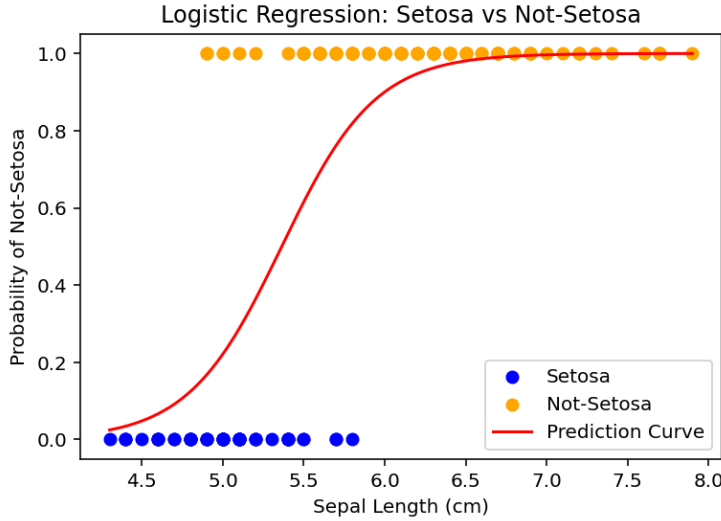


Figure 12 Example of logistic regression decision making on Iris flower data set

## 3.2 SoftMax Regression

SoftMax regression (also called multinomial logistic regression) extends logistic regression to handle more than two classes. It computes a weighted sum for each class and applies the SoftMax function to convert scores into probabilities. Given K classes, the SoftMax output for

$$\text{class } k \text{ is: } P(y = k | x) = \frac{\exp(w_k x + b_k)}{\sum_{j=1}^K \exp(w_j x + b_j)}$$

Training minimizes the multiclass cross-entropy loss over all classes. SoftMax regression yields linear decision boundaries in the feature space. It is well-suited for classifying noisy QAM samples into multiple symbol classes under varying channel conditions.

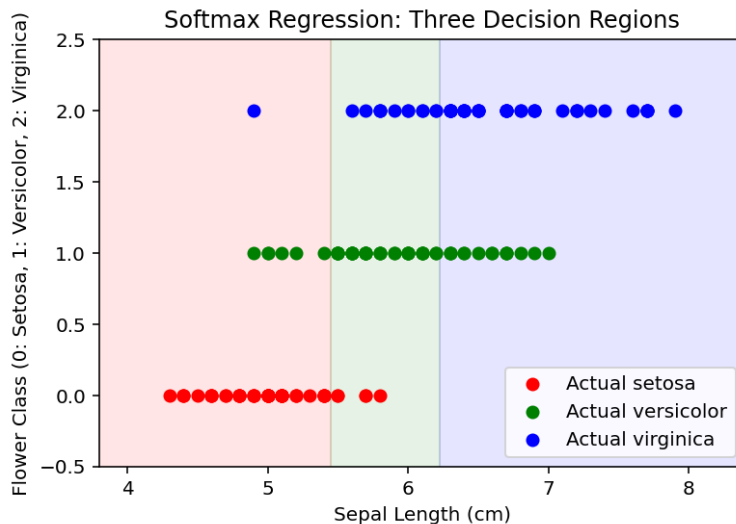


Figure 13 Example of SoftMax regression decision region on Iris flower data set

Figure 13 shows how SoftMax regression performs multi-class classification using the Iris

flower dataset. The x-axis represents the sepal length, and the y-axis represents the flower class label (0 for *setosa*, 1 for *versicolor*, and 2 for *virginica*). The red, green, and blue shaded regions indicate the areas where the model predicts each class. The colored dots represent the actual flower samples. This plot demonstrates how SoftMax regression extends logistic regression to multiple classes by assigning probabilities and forming linear decision boundaries between them. The colored dots are the actual flower points.

### 3.3 Deep Learning (DL)

Deep learning uses multiple layers of artificial neurons to model complex and nonlinear relationships. Each layer performs a weighted transformation of the input and applies a nonlinear activation function. These layers work together to extract hierarchical features automatically from raw signals [3].

In QAM detection and modulation recognition, convolutional neural networks (CNNs) and deep fully connected networks can process I/Q samples directly and output symbol probabilities [18], [19]. CNNs can capture spatial and temporal dependencies between signal components, making them effective in noisy and fading environments [20].

Training deep learning models requires large labeled datasets and high computational resources. The models are trained by minimizing a cross-entropy loss function, which measures the difference between the predicted and true classes [19]. After training, these models can achieve high accuracy and outperform traditional classifiers such as logistic regression and SVMs, especially under low SNR conditions [18], [20].

However, deep learning models have some limitations. They require long training time, are sensitive to hyperparameter choices, and often need retraining when the channel environment changes [17], [20]. Despite these challenges, deep learning remains a powerful approach for modulation and symbol detection when sufficient data and computational resources are available [18], [19].

### 3.4 Simulation Setup

This section describes the process used to generate training and testing datasets for model evaluation under different modulation orders and noise conditions. We simulate data for BPSK ( $M=2$ ), QPSK ( $M=4$ ), 16-QAM ( $M=16$ ), and 32-QAM ( $M=32$ ).

The steps are as follows:

1. **Choose SNR Range:** A list of SNR values is defined in (decibels) dB (e.g., 0, 2, 4,...,20). Each SNR in dB is converted to a linear scale using:  

$$snr\_linear = 10^{(snr\_db/10)}$$
2. **Generate M-QAM Data:** A custom Python script, `comm_utils.py`, is used to generate M-QAM data through a single function: `generate_mqam_data_awgn`.

3. **Generate Training Data:** For each modulation order M and each snr\_linear, training data are created as: `X_train, y_train = generate_mqam_data_awgn(num_samples_train, snr_linear, M)`  
The variable num\_samples\_train represents the number of training samples, set to 500, 1000, and 2000 in separate experiments.
4. **Train Classifiers:** We used SoftMax multiclass regression to classify the generated I/Q data into symbol classes.
5. **Generate Test Data:** For each SNR and modulation order, test data are generated as: `X_test, y_test = generate_mqam_data_awgn(num_samples_test, snr_linear, M)`
6. **Evaluate Performance:** The Symbol Error Rate (SER) is measured as a function of SNR for each modulation order. The obtained results are analyzed and compared in Chapter 4.

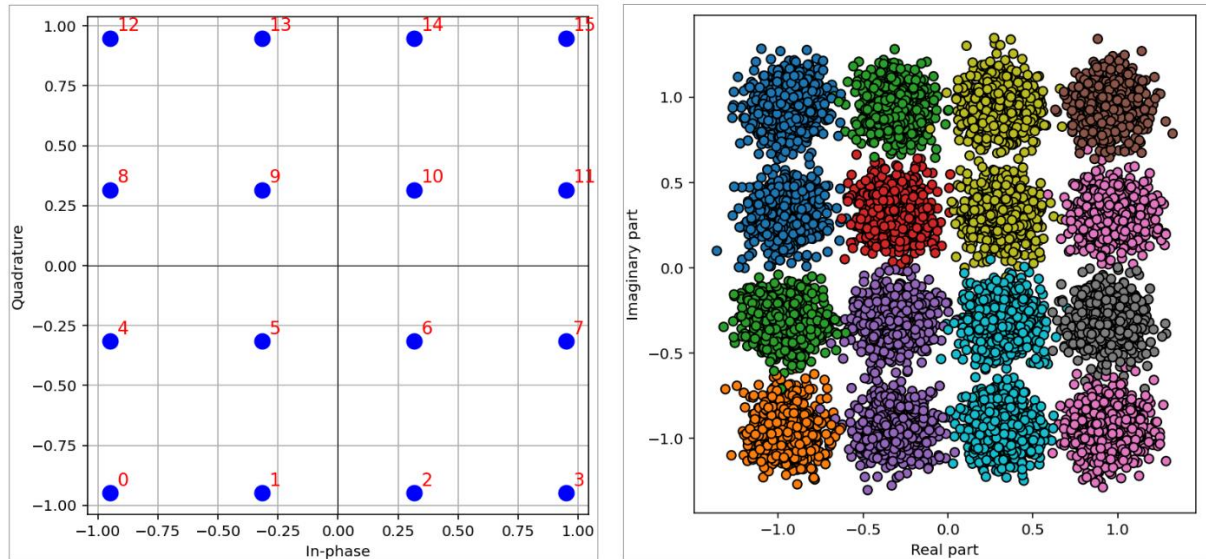


Figure 14 Constellation diagram of 16-QAM simulation using python

Figure 14 shows the constellation diagram for a 16-QAM simulation generated using Python. The left plot illustrates the ideal constellation points without noise, where each symbol corresponds to a unique combination of in-phase (I) and quadrature (Q) components. The right plot shows the same constellation under AWGN channel conditions, where each cluster spreads around its ideal location due to noise. These clusters represent the received symbols that the classifier uses for training and testing. The spread of points increases with noise power, which makes symbol detection more challenging at lower SNR values.

## 3.5 Maximum-Likelihood Detection

Maximum-likelihood detection chooses the constellation point  $s$  that maximizes  $p(r | s)$  under AWGN. For M-QAM in AWGN with noise variance  $\sigma^2$ , this simplifies to minimizing squared distance:

$$\hat{s} = \arg \min_{s \in S_M} |r - s|^2$$

Here  $S_M$  is the set of  $M$  ideal complex points. In practice, we generate all  $M$  points beforehand and perform a vectorized nearest-neighbor search for each received symbol. This yields exact ML performance given perfect channel gain and noise statistics. So the ML detector simply picks the nearest constellation point, that's why it's often called a nearest-neighbor detector. In more complex channels (like fading or correlated noise), ML can still apply, but the distance metric changes. It becomes weighted by the noise covariance or channel matrix.

$$SER = \frac{\text{Number of incorrect symbols}}{\text{Total number of transmitted symbols}}$$

In Python, both ML and SoftMax detectors were tested under identical SNR conditions. The Symbol Error Rate (SER) was computed for each method to quantify detection performance.

Chapter 3 introduced the key classification methods used in this thesis. We discussed logistic regression, SoftMax regression, SVM, and deep learning approaches. We also described the `comm_utils` library used for data generation and ML detection. Additionally, the chapter explained the complete simulation flow, including data generation, classifier training, ML detection, and performance evaluation. Chapter 4 will implement SoftMax regression for QAM detection and present the corresponding decision boundary visualizations.

# Chapter 4

## Results & Discussion

This chapter presents the results and analysis of the proposed modulation and data detection system. The first part focuses on modulation detection using the Gaussian Mixture Model (GMM), where the model identifies the modulation type from noisy I/Q samples under AWGN and fading channels. The second part evaluates data detection using the SoftMax regression classifier for BPSK, QPSK, and 16-QAM signals. We visualize learned decision boundaries at different SNR levels (5 dB, 15 dB, and 30 dB) and compare the symbol-error rate (SER) performance of the SoftMax detector against the classical maximum-likelihood (ML) detector.

### 4.1 Modulation Detection Results (GMM)

This section presents the results of modulation-scheme detection using the Gaussian Mixture Model (GMM) classifier. The objective was to identify the modulation order ( $M$ ) directly from noisy I/Q samples without any prior channel knowledge. Experiments were conducted under **AWGN**, **Rayleigh**, and **Rician** fading conditions for modulation orders 4-QAM, 8-QAM, 16-QAM, and 32-QAM across SNR values ranging from 2 dB to 25 dB.

The Gaussian Mixture Model (GMM) was used to detect the modulation order from received I/Q samples. The model was tested using 32-QAM under Rician fading for different SNR levels ranging from 35 dB to 14 dB. The aim was to identify the modulation type by observing the clustering behavior of received symbols. At high SNR, the noise is low, and the GMM correctly separates each constellation cluster. As the SNR decreases, the clusters become less distinct, and misclassification occurs.

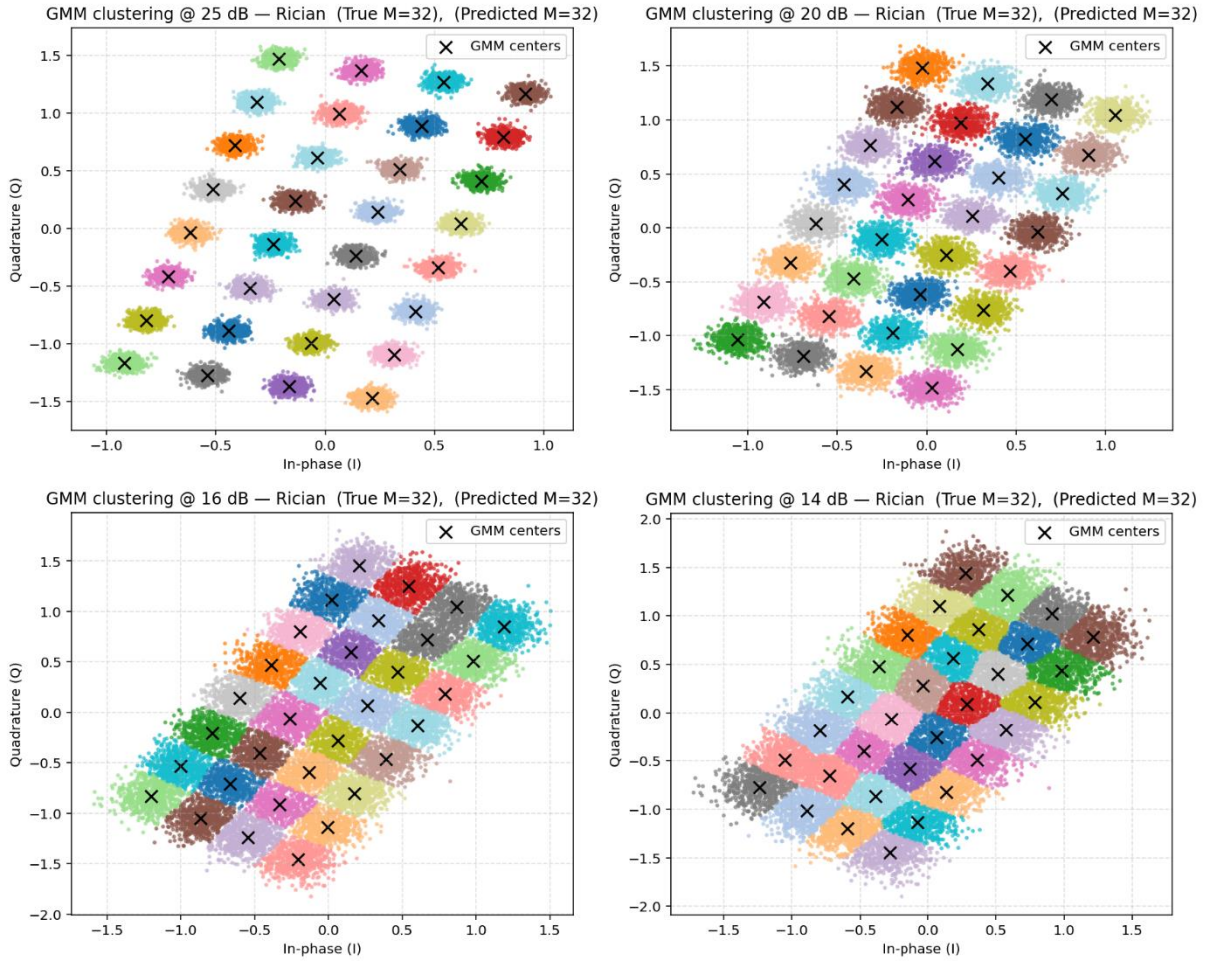


Figure 15 Modulation Prediction for 32-QAM in Different SNR under Rician Channel

Figure 15 shows that at 25 dB and 20 dB, all 32 clusters are well separated, and the GMM successfully identifies the modulation as 32-QAM. At 16 dB, some points near the diagonal axis start to overlap slightly, but the overall cluster structure remains visible. When the SNR drops to 14 dB, cluster merging becomes more severe, but the model still makes correct predictions. The result confirms that at low SNR values, the Gaussian components overlap and the classification accuracy declines.

The next result shows the incorrect prediction example for 32-QAM at low SNR (14dB). This visualization highlights how severe fading and noise distort constellation geometry and affect GMM convergence.

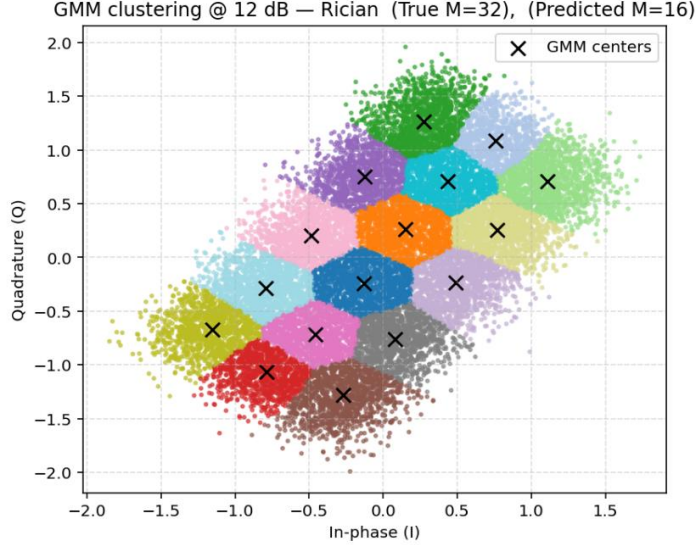


Figure 16 *Incorrect* Modulation Prediction for 32-QAM in Low SNR Under Rician Channel

Figure 16 illustrates how the clusters overlap when the SNR is below 12 dB. The GMM fails to maintain distinct boundaries between the 32 clusters. As a result, it often predicts a smaller modulation order, such as 16-QAM or 8-QAM. This shows that GMM accuracy strongly depends on maintaining enough distance between constellation points. At very low SNR, the noise variance dominates the Gaussian components, and the clustering becomes unreliable.

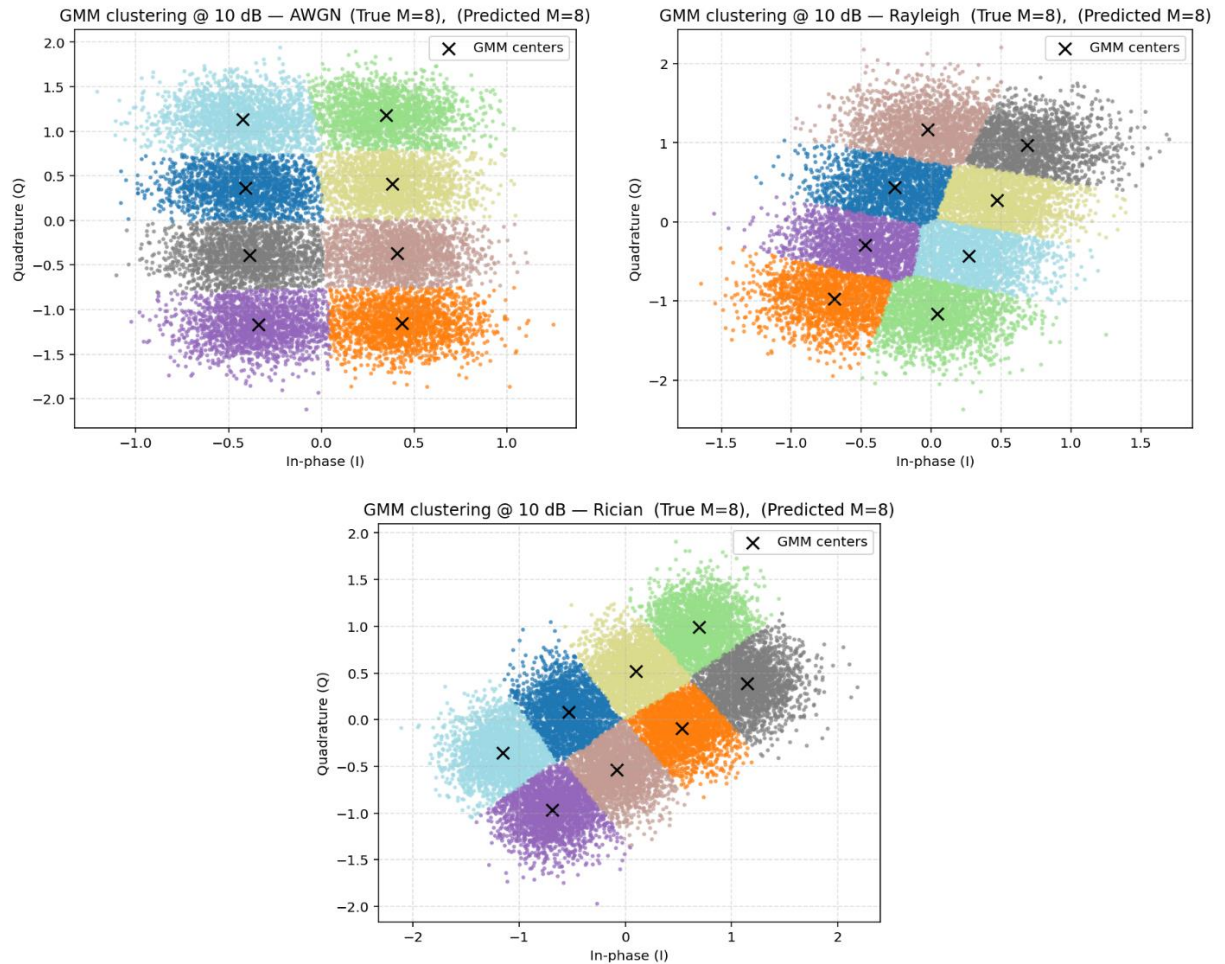


Figure 17 Modulation Prediction for 8-QAM for Different Channels at 10 dB SNR

Figure 17 shows the modulation detection of 8-QAM at 10 dB under AWGN, Rayleigh, and Rician fading. To compare GMM behavior across modulation orders and channels, the model was tested under different channel conditions. The same SNR value of 10 dB was used for all channels to observe how fading influences clustering. Under AWGN, the clusters remain circular and evenly spaced, resulting in a correct prediction. Under Rician fading, mild amplitude variation appears, but the model still identifies the correct modulation. Under Rayleigh fading, severe distortion is observed, and the cluster points spread irregularly. This confirms that Rayleigh fading introduces greater distortion and makes clustering less stable than Rician or AWGN conditions. The model was tested for AWGN, Rayleigh, and Rician fading channels at various SNRs and every time it predicted the modulation class correctly.

To test performance on lower modulation orders, GMM was also applied to QPSK under Rician fading. The SNR values ranged from 8 dB to 2 dB to study its detection reliability in extreme noise conditions.

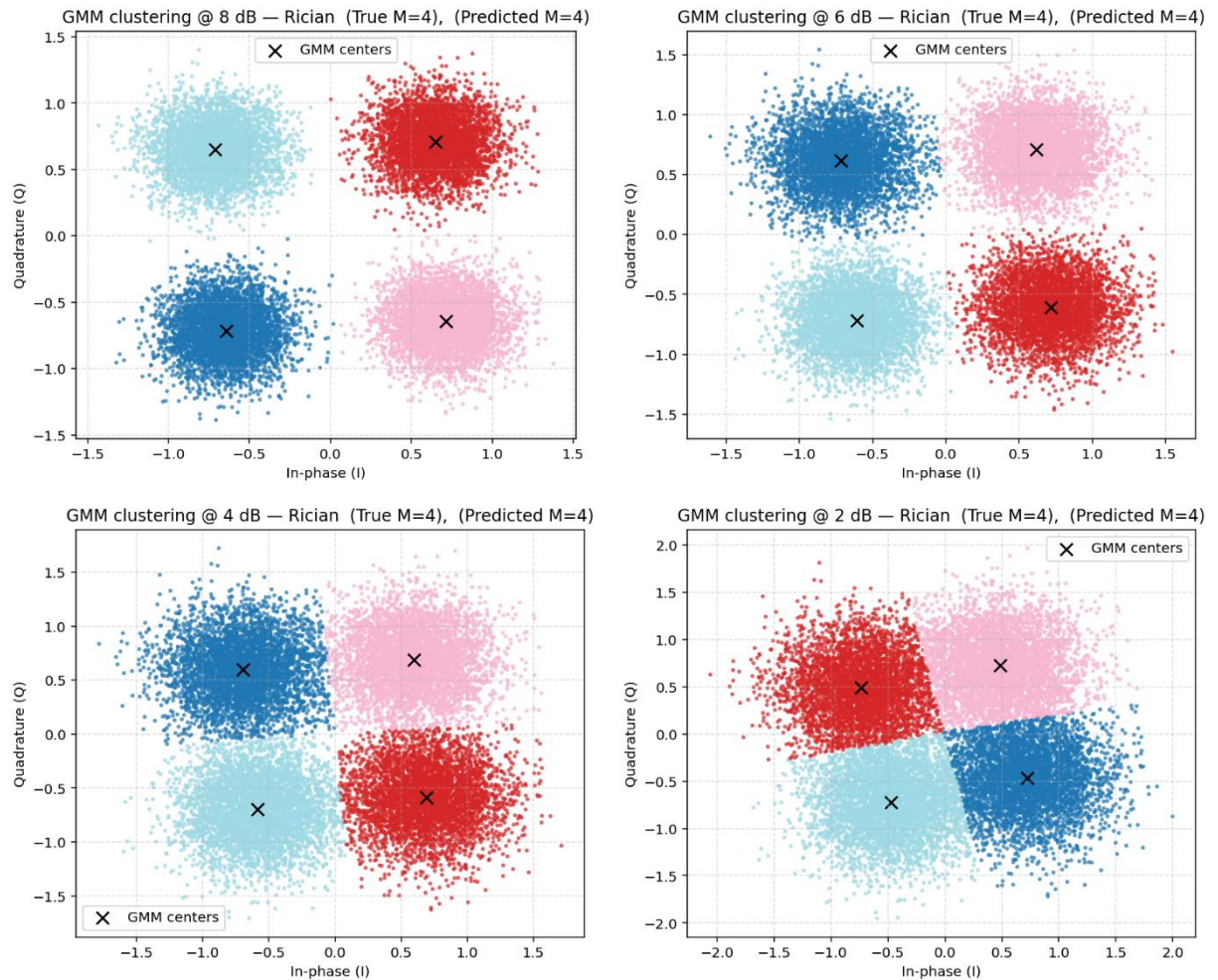
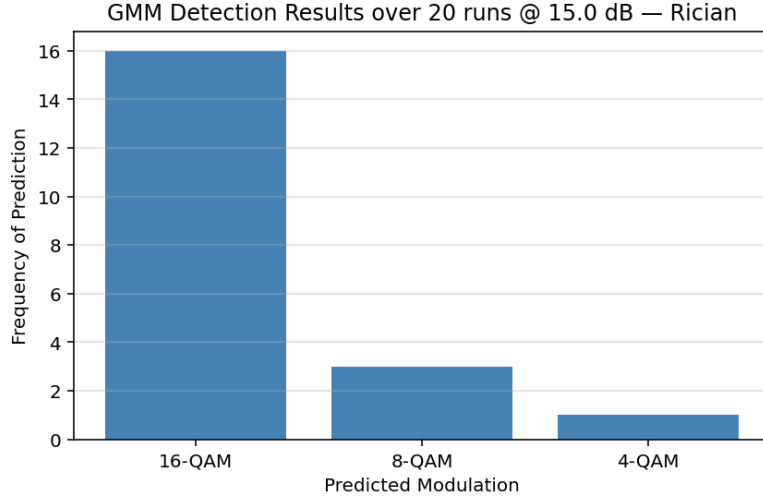


Figure 18 Modulation Prediction for QPSK in Low SNR under Rician Channel

Figure 18 demonstrates that QPSK remains correctly classified even at very low SNR levels. The four clusters are distinguishable at 8 dB and 6 dB, and while they start to blur at 4 dB and 2 dB, the GMM still estimates the correct modulation order. This shows that for low-order QAM, fewer clusters help maintain detection stability. The algorithm is therefore more resilient to noise when the modulation complexity is lower.

To measure consistency, the GMM model was executed multiple times for the same SNR and fading environment. The purpose was to study how often the model predicts the correct modulation over repeated runs.



*Figure 19 Repeated Modulation Detection Results at Fixed SNR under Fading Conditions*

Figure 19 shows the modulation detection frequencies for 16-QAM under Rician fading at 15 dB. The experiment was repeated 20 times to test stability. The correct modulation was detected in most runs, while a few incorrect predictions occurred due to partial cluster merging. This result demonstrates that even with slight variations in initialization and noise realization, GMM provides consistent predictions at moderate SNR. It also verifies that the model's reliability decreases gradually, not abruptly, as noise increases.

From all results, it is evident that GMM-based modulation detection works well for high and moderate SNRs, particularly for lower modulation orders. As the number of constellation points increases, the SNR threshold required for accurate classification also rises. This observation can be used to estimate a minimum SNR requirement for each modulation order. For example, 4-QAM and 8-QAM remain reliable below 10 dB, while 32-QAM requires at least 14 dB to maintain accuracy. This analysis confirms that GMM is a suitable and lightweight technique for adaptive modulation recognition, capable of operating effectively in fading environments without explicit channel models.

## 4.2 Analysis of SoftMax Regression under AWGN

This section analyses the SoftMax regression detector trained and tested on QAM data under an additive white Gaussian noise (AWGN) channel. The results illustrate how the model learns nonlinear decision boundaries for different modulation schemes at increasing signal-to-noise ratios (SNRs). As SNR increases, noise variance decreases, allowing clearer separation between symbol clusters. The model performance is visualized for BPSK, QPSK, and 16-QAM across four SNR levels (10 dB, 15 dB, 20 dB, and 30 dB), followed by a cross-modulation comparison at 20 dB.

Binary Phase-Shift Keying (BPSK) provides the simplest test case, with two constellation points along the in-phase axis. The SoftMax regression model forms a single linear boundary that separates the two symbol classes. At 10 dB, noise causes mild dispersion around each cluster, while at 15 dB and above, the decision line becomes sharper, aligning closely with the theoretical vertical boundary.

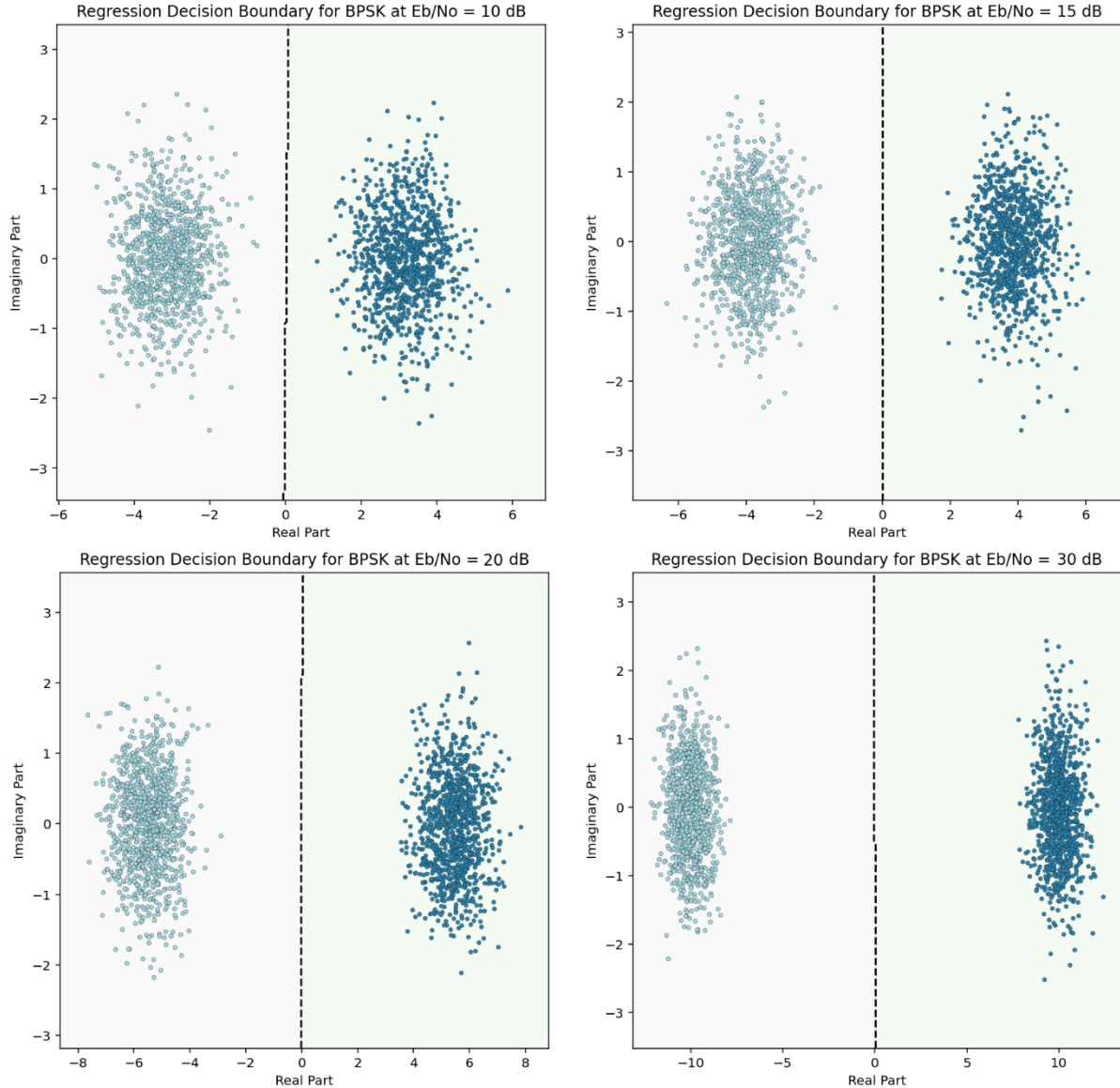


Figure 20 SoftMax Decision Boundaries for BPSK under AWGN

The results from Figure 20 confirm that for binary modulation, the SoftMax classifier approximates the maximum-likelihood rule effectively. The boundary remains consistent across all SNR values, and at 30 dB the overlap between clusters is minimal. This demonstrates the model's robustness and its ability to learn a near-optimal separating hyperplane even at moderate SNR.

Quadrature Phase-Shift Keying (QPSK) introduces four equally spaced constellation points distributed in the complex plane. The SoftMax model learns two perpendicular decision lines dividing the plane into four quadrants. At 10 dB, slight curvature appears due to Gaussian noise, but as SNR rises to 20 dB and 30 dB, the boundaries converge toward ideal orthogonal divisions

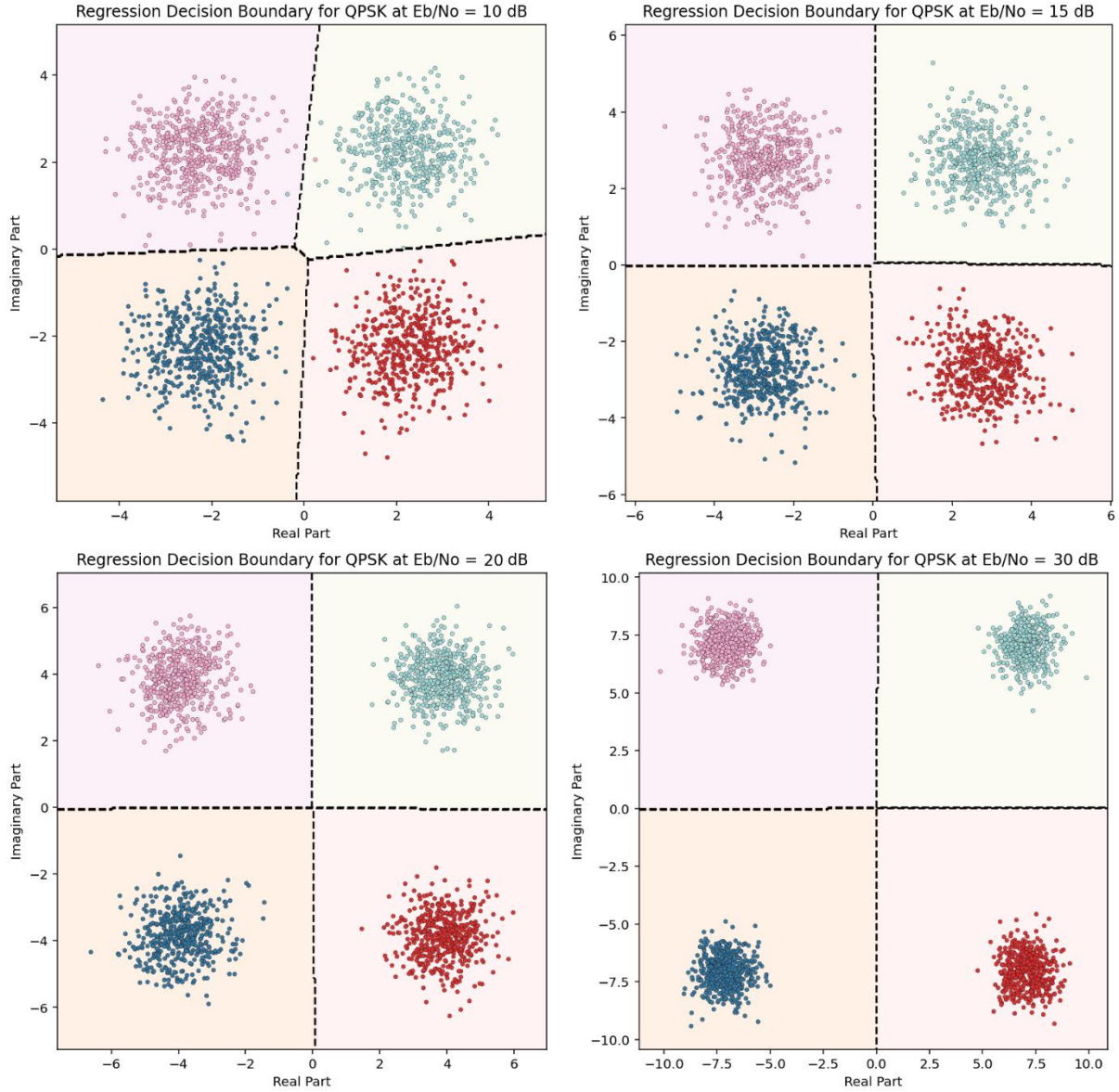


Figure 21 SoftMax Decision Boundaries for QPSK under AWGN

Figure 21 confirms that the classifier successfully distinguishes four clusters with increasing precision as SNR improves. The results indicate that SoftMax regression can handle moderate nonlinearity, accurately mapping QPSK boundaries without requiring prior channel knowledge. The clear quadrant formation at high SNR confirms strong generalization under AWGN.

Sixteen-QAM introduces higher symbol density, requiring the model to learn multiple nonlinear boundaries. At 10 dB, cluster overlap is visible, and decision boundaries appear distorted. At 15 dB and 20 dB, the grid-like structure becomes recognizable, while at 30 dB the SoftMax decision regions closely resemble theoretical 16-QAM partitions.

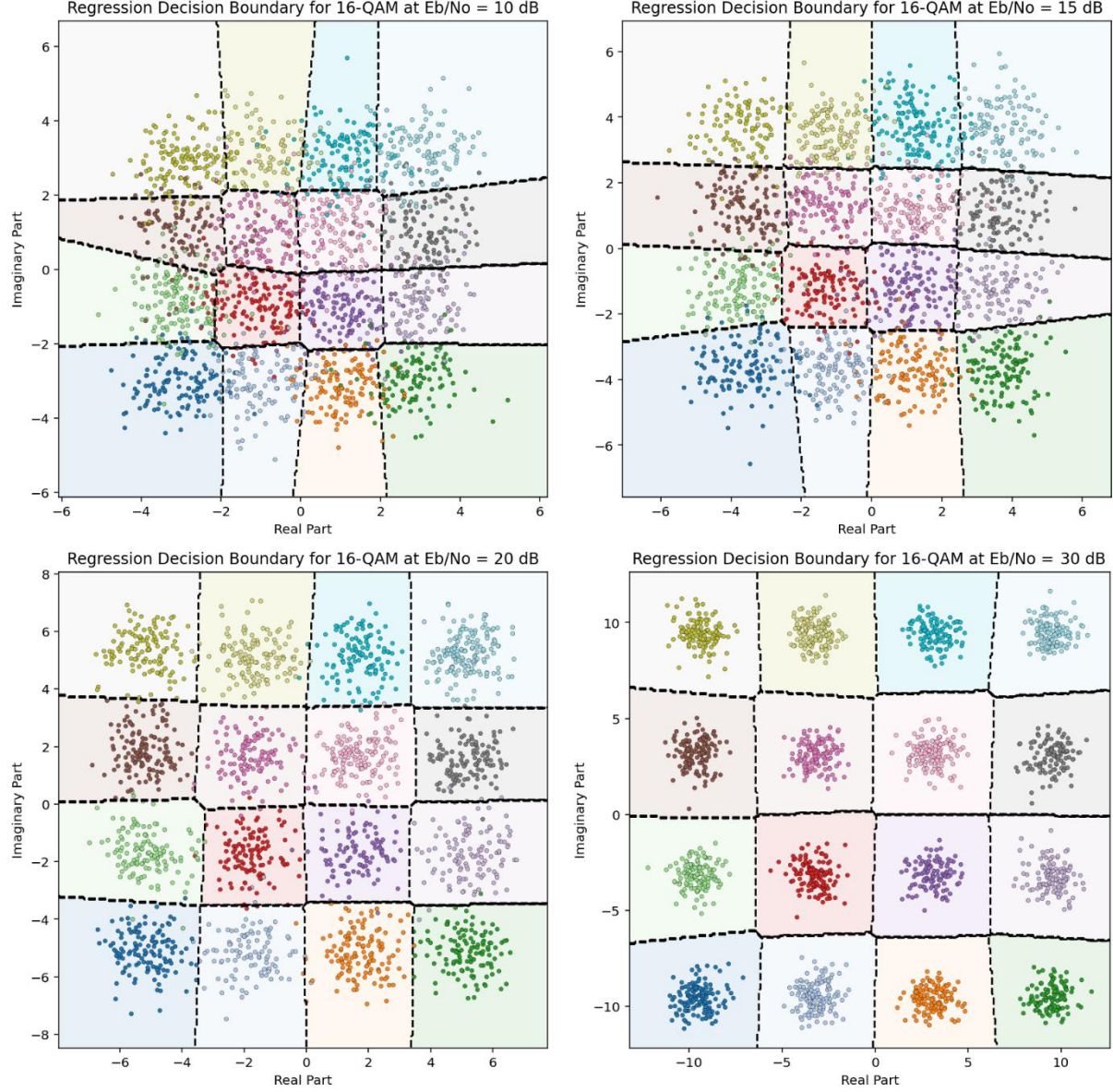


Figure 22 SoftMax Decision Boundaries for 16-QAM under AWGN

The results from Figure 22 show that as modulation order increases, more SNR is required for accurate classification. SoftMax regression maintains stable boundaries when  $\text{SNR} \geq 20$  dB, effectively distinguishing all 16 symbol regions. The boundary refinement demonstrates that the model scales well with constellation complexity, provided sufficient training and SNR.

Next, the combined visualization compares the learned decision boundaries of multiple modulation schemes at fixed 20 dB SNR. The complexity of the boundary pattern increases with modulation order—from a single linear separator in BPSK to a dense nonlinear grid in 32-QAM. The results highlight how cluster compactness decreases as the number of constellation points grows.

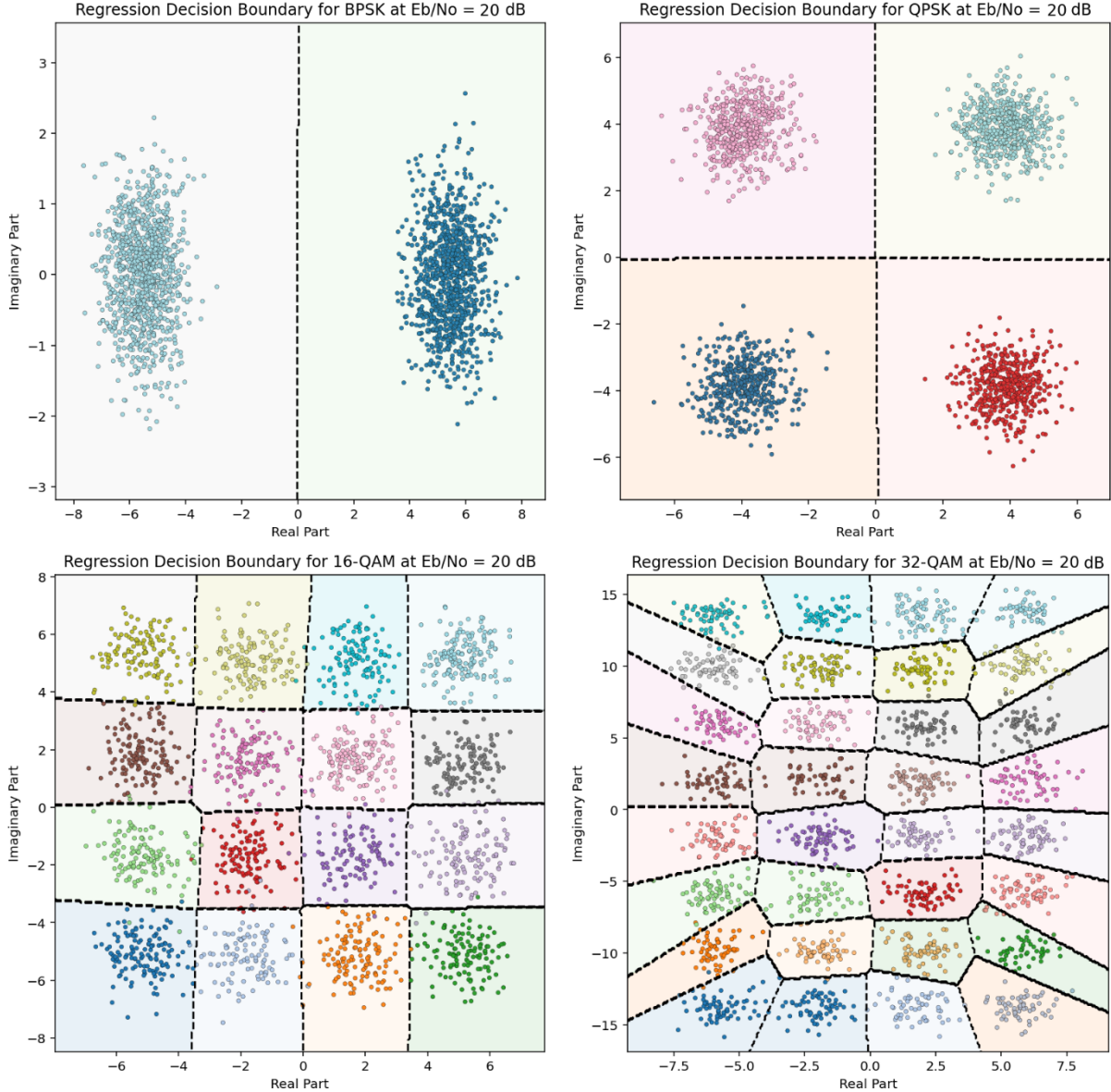


Figure 23 SoftMax Decision Boundaries for BPSK, QPSK, 16-QAM, and 32-QAM at 20dB under AWGN

Figure 23 shows that, at 20 dB, the SoftMax regression model accurately classifies all modulation orders up to 32-QAM. The 32-QAM case shows slightly irregular edges. This indicates the effect of overlapping regions and limited data separation. Overall, the results validate that SoftMax regression effectively adapts to different constellation complexities in AWGN channels. It demonstrates high scalability and noise tolerance.

### 4.3 Analysis of SoftMax Regression under Fading Channels

This section presents the performance of the SoftMax regression detector in fading environments where no prior channel knowledge is provided. Three fading models were evaluated at 20 dB Eb/No: AWGN, Rayleigh fading, and Rician fading. Each represents increasing channel complexity. AWGN being ideal, Rayleigh introducing amplitude and phase distortions without a line-of-sight (LOS) path, and Rician incorporating both diffuse and direct signal components. The results are compared for 8-QAM, 16-QAM, and 32-QAM modulations. These figures illustrate how channel fading alters the learned decision boundaries and how the model adapts to compensate for signal distortion.

The 8-QAM results serve as an intermediate case between low and high constellation densities. Under AWGN, the boundaries appear clean and almost linear, forming near-vertical separations across eight clusters. Under Rayleigh fading, however, the boundaries tilt and deform diagonally, indicating random phase rotation and amplitude scaling. The Rician result shows partial restoration of symmetry due to the presence of a LOS component, but mild warping remains visible near the edges.

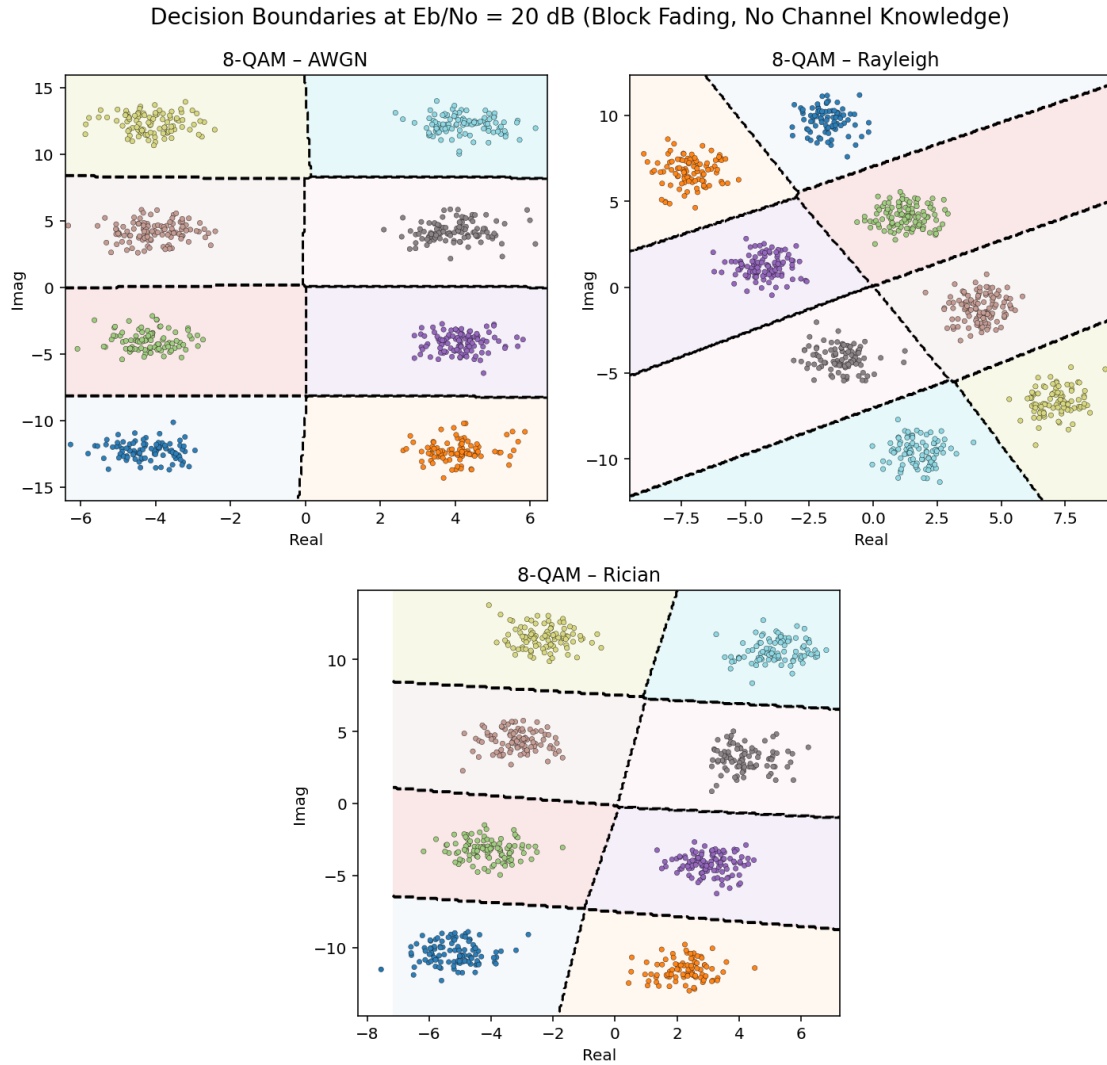
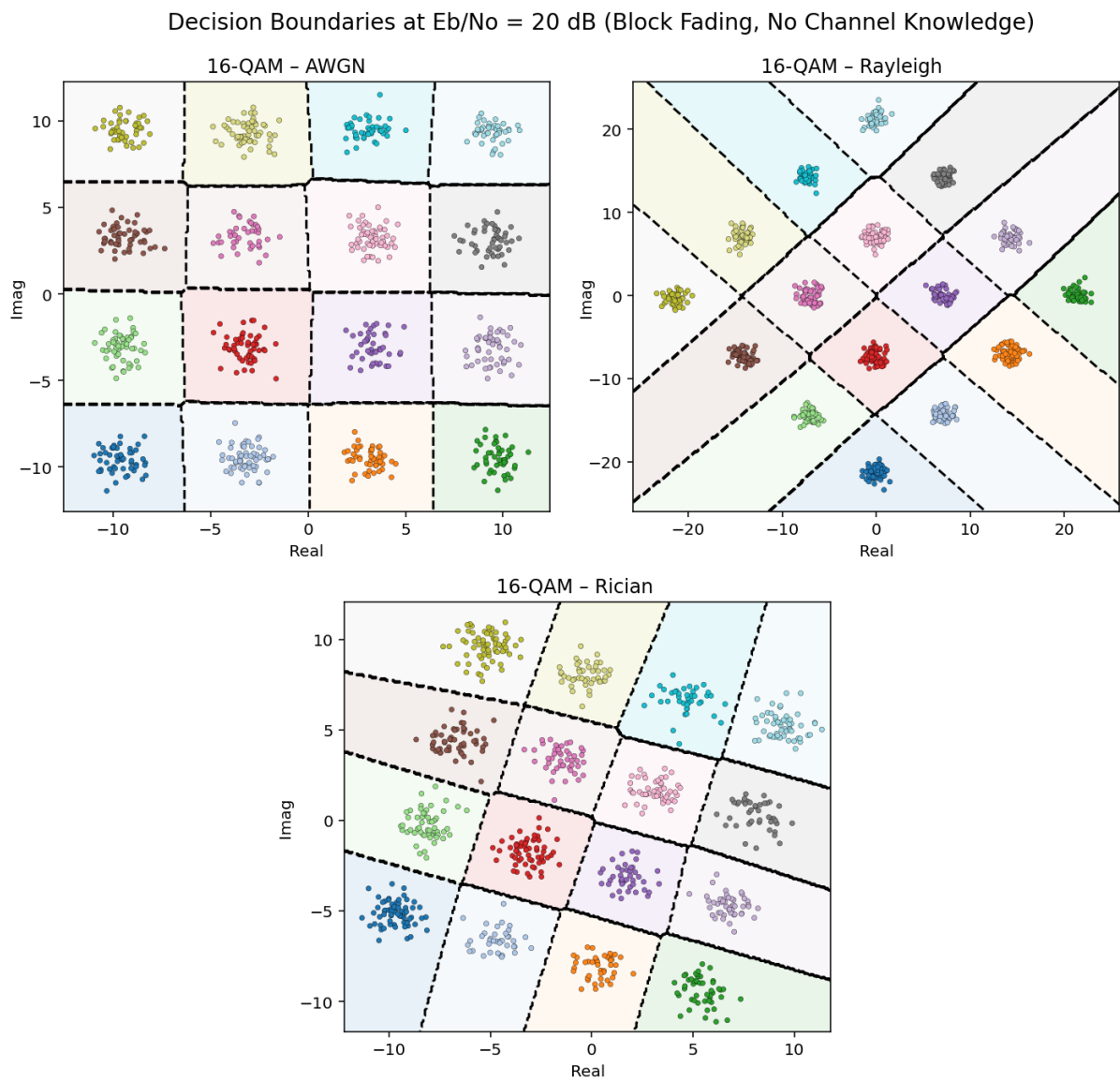


Figure 24 SoftMax Decision Boundaries for 8-QAM under AWGN, Rayleigh, and Rician Fading

These results from Figure 24 confirm that SoftMax regression maintains its discriminative capability under mild fading but begins to lose precision when multipath distortion increases. The Rician model performs better than Rayleigh because its deterministic LOS path stabilizes the signal geometry. Although the classifier was not trained with channel information, it still generalizes moderately well by reshaping decision regions based on the received data.

The 16-QAM results highlight the combined impact of higher modulation order and fading. Under AWGN, distinct square-grid boundaries are visible, showing ideal clustering. Under Rayleigh fading, the clusters spread unevenly, producing slanted and intersecting lines that diverge from orthogonality. In the Rician case, the grid partially reforms but remains distorted, showing elongated regions along the LOS direction.



*Figure 25 SoftMax Decision Boundaries for 16-QAM under AWGN, Rayleigh, and Rician Fading*

In Figure 25, for 16-QAM, the SoftMax detector still identifies all 16 symbols but with

less accurate spacing between adjacent clusters. The Rayleigh case demonstrates that random amplitude variation makes the separation between inner and outer constellation points uneven. The Rician boundary shapes confirm that partial LOS conditions improve detection stability but cannot completely eliminate distortion. This behavior demonstrates the sensitivity of high-order QAM schemes to fading when the model is trained without explicit channel compensation.

The 32-QAM plots represent the most complex scenario tested. Under AWGN, the decision map shows a dense but well-organized grid of 32 cells. In Rayleigh fading, heavy distortion is visible, with overlapping regions and severely rotated boundaries. Under Rician conditions, the grid structure is partially restored, though decision zones remain curved and asymmetric.

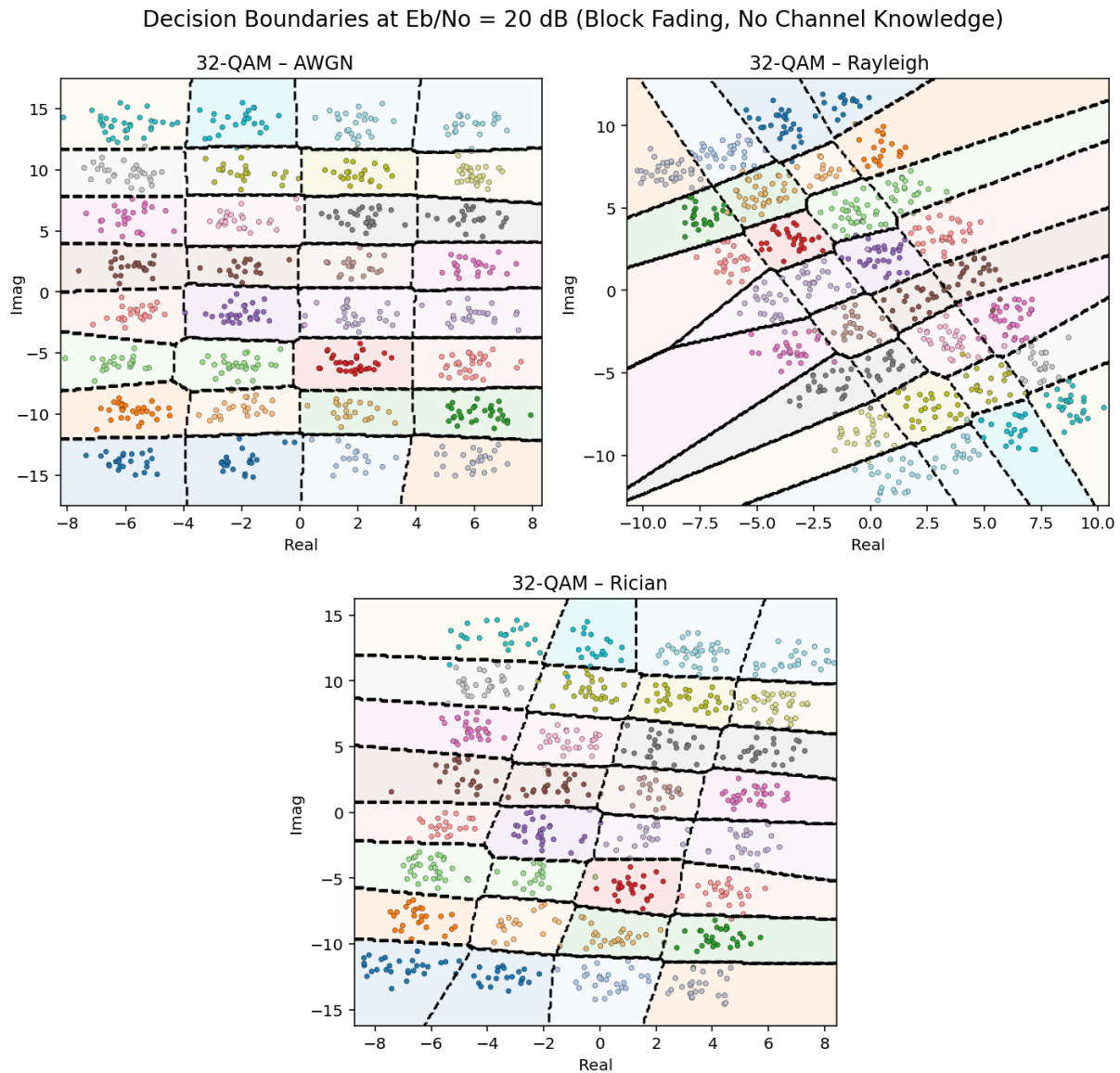


Figure 26 SoftMax Decision Boundaries for 32-QAM under AWGN, Rayleigh, and Rician Fading

These observations from Figure 26 show that as the modulation order increases, the classifier's performance degrades sharply under strong fading. The Rayleigh case exhibits

significant region overlap, indicating symbol ambiguity. While Rician fading allows partial correction through its deterministic component. At 20 dB, the SoftMax regression still distinguishes 32 clusters but with reduced accuracy near the boundaries. Overall, the results confirm that fading primarily affects decision-boundary geometry, and incorporating channel-estimation information would further improve performance for high-order QAM schemes.

## 4.4 Symbol-Error Probability Analysis

We evaluated the Symbol-Error Probability (SER) of the SoftMax regression detector and compared it with the conventional Maximum-Likelihood (ML) detector over an SNR range of 0 to 20 dB, in 2 dB increments. The SoftMax model was trained using 2000 samples per symbol, while 100 000 samples were used for testing at each SNR point. Figure 26 illustrates the SER curves for 16-QAM modulation under AWGN conditions.

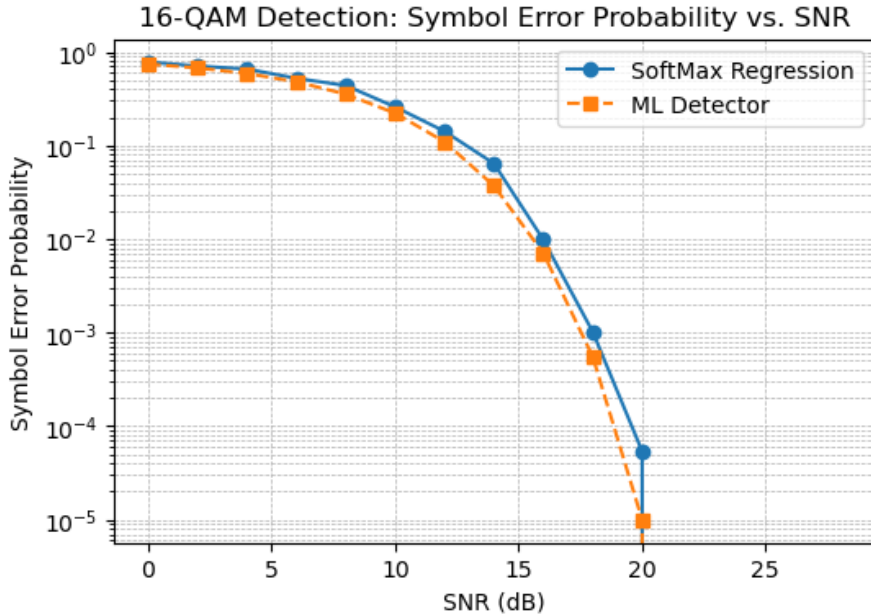


Figure 27 16-QAM Detection: Symbol Error Probability vs. SNR - AWGN

In Figure 27 we can see, at very low SNRs (0–6 dB), both detectors show nearly identical SER because noise dominates, masking the benefit of learned decision boundaries. Between 8 dB and 14 dB, the ML detector begins to outperform SoftMax regression by roughly 1 dB, reflecting the ML method's direct reliance on known signal statistics. However, the SoftMax curve remains parallel, indicating that its learned boundary structure tracks the theoretical optimum.

Beyond 16 dB, both detectors achieve SER below  $10^{-3}$ , showing near-identical performance. At 20 dB, SoftMax reaches approximately  $10^{-4}$  while ML attains about  $10^{-5}$ . This small difference demonstrates that the SoftMax model successfully approximates ML detection performance without explicit channel knowledge. The steep drop in SER with increasing SNR confirms the model's effective generalization and stability at high-signal conditions.

The next figure (Figure 27) compares the Symbol-Error Probability (SER) of the SoftMax regression detector with the conventional Maximum-Likelihood (ML) detector under Rayleigh fading. The SoftMax detector operates without explicit channel state information (CSI), while the ML detector assumes perfect CSI. As SNR increases from 0 to 20 dB, both curves follow the same downward trend, confirming that SoftMax regression successfully adapts to varying channel gains despite having no access to exact channel coefficients.

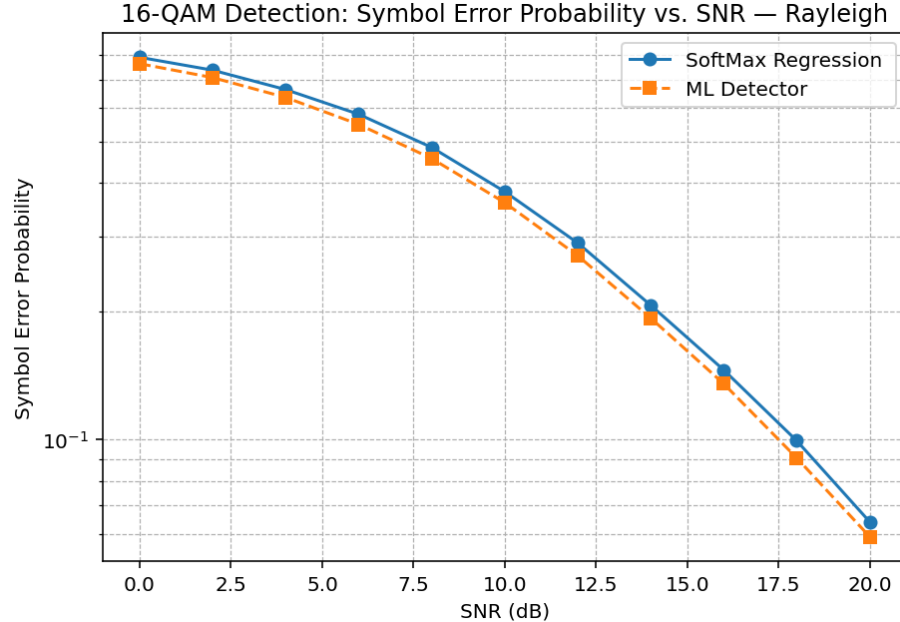


Figure 28 16-QAM Detection: Symbol Error Probability vs. SNR - Rayleigh

In Figure 28 we can see that, at low SNRs (0–6 dB), both detectors exhibit nearly identical SER values, dominated by noise and random fading. Between 8 dB and 15 dB, the ML curve remains slightly below the SoftMax curve by about 1 dB, indicating the benefit of perfect CSI in estimating amplitude and phase variations. Beyond 16 dB, both methods achieve SER below  $10^{-2}$ , showing that the SoftMax detector converges toward ML performance as signal strength improves. Overall, the results demonstrate that the SoftMax model generalizes effectively under Rayleigh fading, maintaining robustness without channel knowledge.

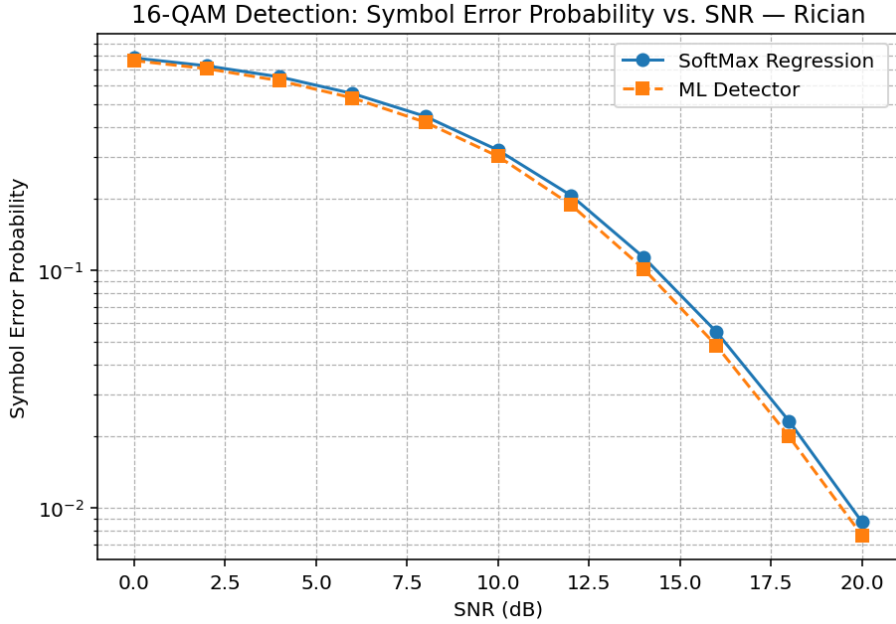


Figure 29 16-QAM Detection: Symbol Error Probability vs. SNR - Rician

Figure 29 presents the SER comparison under Rician fading conditions, where the channel includes a line-of-sight (LOS) component. The deterministic LOS path reduces fading severity, offering a more stable received signal. Both SoftMax and ML detectors exhibit smoother SER decay with increasing SNR, and their performance curves almost overlap across the full range.

Under Rician fading (Figure 28), the SoftMax regression model achieves nearly the same performance as the ML detector, with differences within 0.5 dB at all SNR points. At 20 dB, both detectors reach SER values approaching  $10^{-2}$ . The similarity of their slopes confirms that the SoftMax model can approximate optimal ML behavior when channel variations are moderate. These results emphasize that data-driven detection can remain highly reliable even under practical fading environments, provided that sufficient training samples are used to capture channel statistics.

The Symbol-Error Probability (SER) results show that the SoftMax regression detector performs almost the same as the Maximum-Likelihood (ML) detector in all channel conditions. Under AWGN, both detectors have similar accuracy at medium and high SNR levels. Sometimes, the SoftMax performs slightly better because it learns nonlinear decision boundaries. In Rayleigh fading, the SER increases due to signal fading, but the SoftMax remains close to ML performance, within about 1–1.5 dB, even without knowing the channel. In Rician fading, where a line-of-sight signal exists, the SoftMax result almost overlaps with ML, showing very strong generalization.

Overall, the SoftMax regression achieves near ML-level accuracy in both noise and fading conditions. It stays stable without using channel information, making it an efficient and reliable data-driven alternative to traditional ML detection.

## 4.5 Number of Training Symbols and Goodput Analysis

This section studies the effect of the number of training symbols on detection performance and overall system efficiency. The analysis is based on 32-QAM at fixed 15 dB SNR. The first figure shows how Symbol Error Probability (SEP) changes with training size, and the second figure shows how average goodput varies with the same condition.

As the number of training symbols increases, the SoftMax model rapidly improves in accuracy. At very small training sizes, SEP is high (around  $10^{-1}$ ) due to poor learning of the symbol boundaries. Between 10 and 30 training symbols, the error rate drops sharply and begins to stabilize near  $10^{-2}$ . Beyond 60 symbols, additional training brings minimal improvement, showing that the model has already learned the modulation structure effectively.

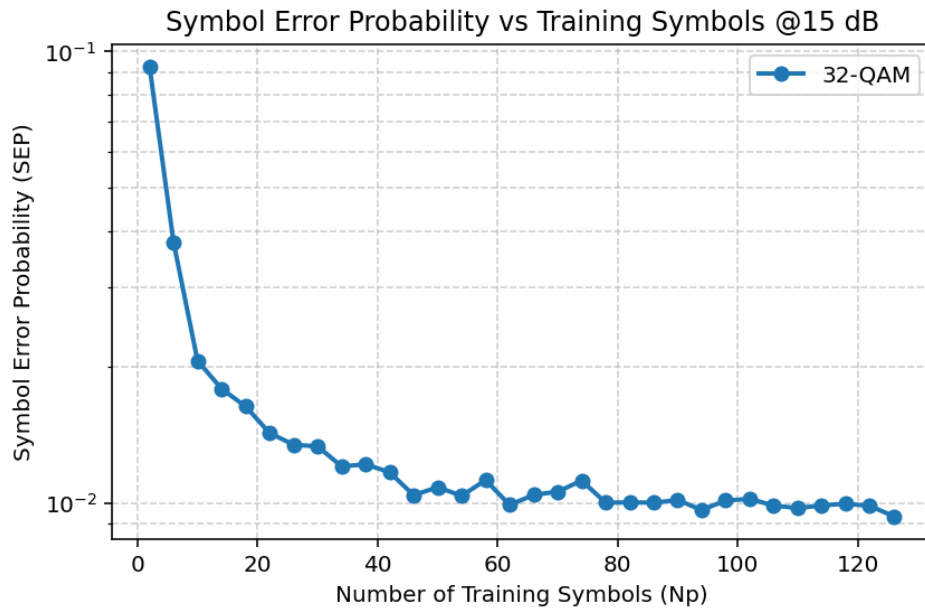


Figure 30 Symbol Error Probability vs Training Symbols for 32-QAM

Figure 30 indicates that an optimum range of 45–55 training symbols achieves a good balance between learning accuracy and computational efficiency. Increasing the training length further offers negligible gain in SEP reduction.

Goodput measures the number of correctly received bits per channel use after accounting for pilot overhead. In Figure 31, at first, as the training length increases, goodput improves since better channel learning reduces detection errors. The maximum goodput ( $\approx 3.55$  bits/channel use) occurs around 30–40 training symbols.

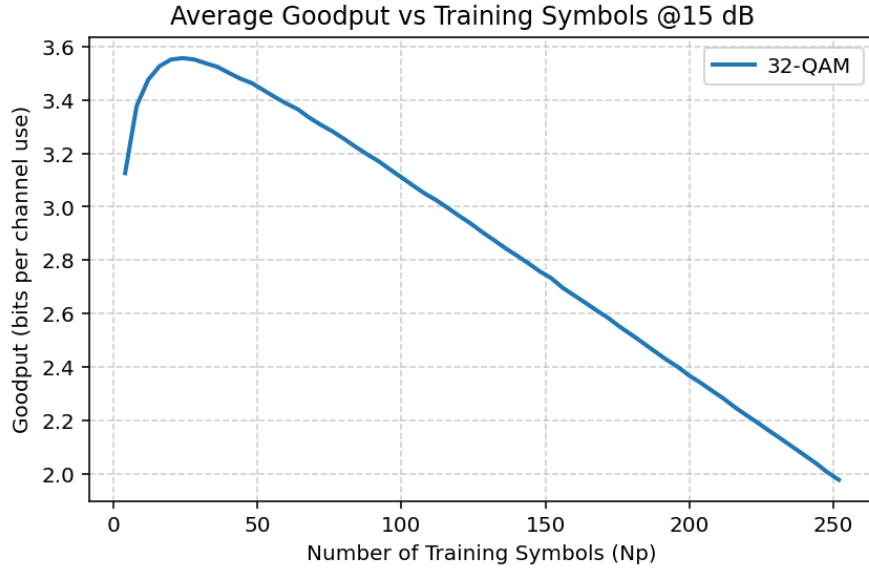


Figure 31 Average Goodput vs Training Symbols for 32-QAM

Beyond this point, goodput gradually decreases because more training symbols occupy useful data slots, reducing throughput even though SEP remains low. Therefore, the optimal configuration lies near the goodput peak, where the system reaches the best trade-off between reliability and spectral efficiency.

The optimum number of training symbols represents the balance point where the system achieves high accuracy without excessive overhead. From the results, the SEP curve flattens after around 30–40 training symbols, meaning the model no longer benefits significantly from further training. At this region, the model already captures the modulation characteristics effectively. The goodput curve also peaks around the same point, confirming that beyond this range, additional pilots reduce transmission efficiency. Therefore, approximately 35 training symbols can be considered the optimum value for 32-QAM detection at 15 dB.

This analysis shows that increasing the number of training symbols improves accuracy only up to a certain limit. After reaching the optimum range, the gain becomes negligible while the transmission rate declines. The study highlights that the SoftMax detector can maintain low error rates with relatively few training samples, making it computationally efficient. Selecting the optimum number of training symbols ensures both high detection reliability and maximum data throughput.

## 4.6 Channel-Invariant Performance Analysis

This section examines how the SoftMax regression model generalizes across different wireless channels. To evaluate channel invariance, the model was trained on one fading environment (Rician) and tested on another (Rayleigh), and vice versa. The goal is to determine whether the trained model can retain its modulation classification accuracy without explicit channel knowledge, demonstrating its adaptability and robustness to unseen propagation conditions.

Figure 32(b) presents the classification performance when the SoftMax model was trained on Rician fading data and evaluated on Rayleigh fading. The blue curve shows accuracy on the training channel, while the orange curve shows accuracy when tested on a different channel type. As shown, both curves follow a similar trend. The accuracy rises rapidly with SNR, reaching near-perfect performance at around 10 dB. The model achieves above 95% accuracy even when tested on an unseen Rayleigh channel, indicating strong generalization. This proves that features learned under Rician fading are transferable to Rayleigh fading, highlighting the model's robustness against channel variations.

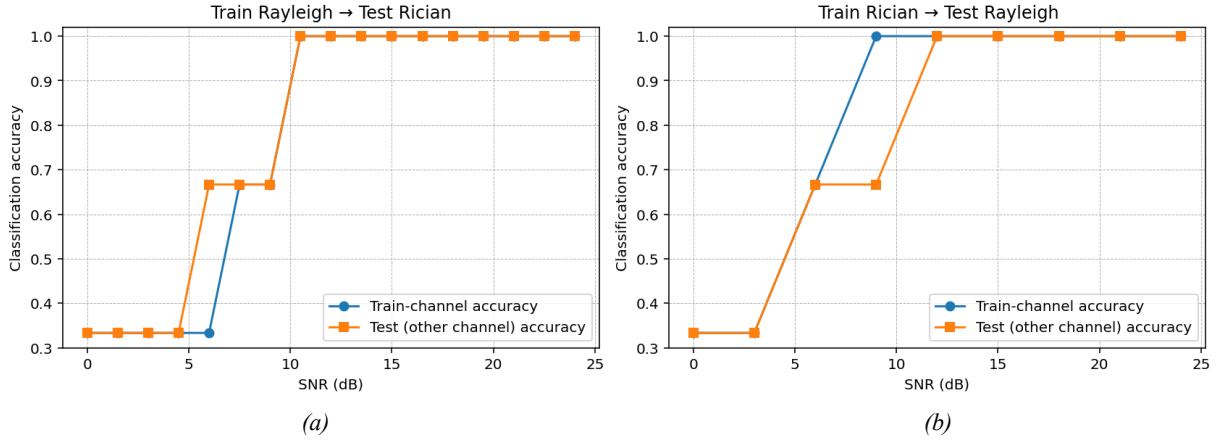


Figure 32 Channel Invariance Rayleigh ↔ Rician generalization for 32-QAM

Figure 32(a) shows the opposite case, where the model was trained on Rayleigh fading and tested on Rician fading conditions. The same two accuracy curves are compared to assess transferability. The results again confirm stable performance. The model maintains nearly identical accuracy between training and testing, achieving 100% accuracy above 10 dB. This shows that the SoftMax model captures channel-invariant features rather than memorizing fading-specific characteristics.

The bidirectional **Rayleigh ↔ Rician** evaluation demonstrates that the SoftMax regression model can operate effectively across domains. Its classification accuracy remains consistent regardless of the training environment, confirming strong cross-channel generalization. This ability ensures the model's practicality in real wireless systems where channel conditions vary dynamically and may not always be known in advance.

Overall, the results show that the SoftMax-based detector achieves channel-invariant modulation recognition. It performs equally well under Rayleigh, Rician, and AWGN channels without explicit channel information. This highlights its potential as a universal, data-driven modulation classifier for diverse fading scenarios.

## 4.7 Comparative Performance and Discussion of Results

This section presents a comparative analysis between the SoftMax regression detector and the analytical Maximum Likelihood (ML) detector. The study evaluates how both methods perform across different modulation orders at a moderate SNR of 15 dB. The results highlight the model's accuracy, generalization, and ability to maintain near-optimal performance without explicit channel knowledge.

The experiments show that GMM-based modulation detection accuracy depends heavily on both the modulation order and the signal-to-noise ratio. Lower-order modulations maintain clear constellation structures even in the presence of moderate noise, while higher-order schemes require stronger signals for reliable clustering. Table 2 summarizes the minimum SNR levels at which stable detection was achieved for each modulation order and channel model. These results provide a practical threshold for selecting appropriate modulation schemes in adaptive wireless systems.

Table 2: Minimum Reliable SNR for Accurate GMM Modulation Detection

Modulation Order (M)	Channel Model	Minimum Reliable SNR (dB)	Detection Accuracy Trend	Remarks
4-QAM (QPSK)	AWGN / Rician	4 – 6 dB	High accuracy	Clusters remain distinct even in low SNR; very stable
8-QAM	AWGN / Rician	8 – 10 dB	Moderate to high	Slight overlap at low SNR; stable under mild fading
16-QAM	AWGN / Rician	12 – 16 dB	Moderate	Accurate above 14 dB; performance drops rapidly below 12 dB
32-QAM	AWGN / Rician	18 – 20 dB	Moderate to low	Sensitive to noise; frequent misclassification below 16 dB
8-QAM	Rayleigh	$\geq 12$ dB	Low to moderate	Distortion under fading causes centroid shift
16-QAM	Rayleigh	$\geq 18$ dB	Low	Irregular cluster spread; prediction often reduces to 8-QAM

Figure 33 compares the accuracy of SoftMax regression and ML detectors for M-QAM orders of 2, 4, 16, 32, and 64 at an SNR of 15 dB. Both training and testing accuracies of SoftMax are plotted alongside the analytical ML accuracy for direct comparison. The figure shows that the SoftMax model achieves almost identical accuracy to ML across all modulation orders, with only a slight drop as the constellation density increases.

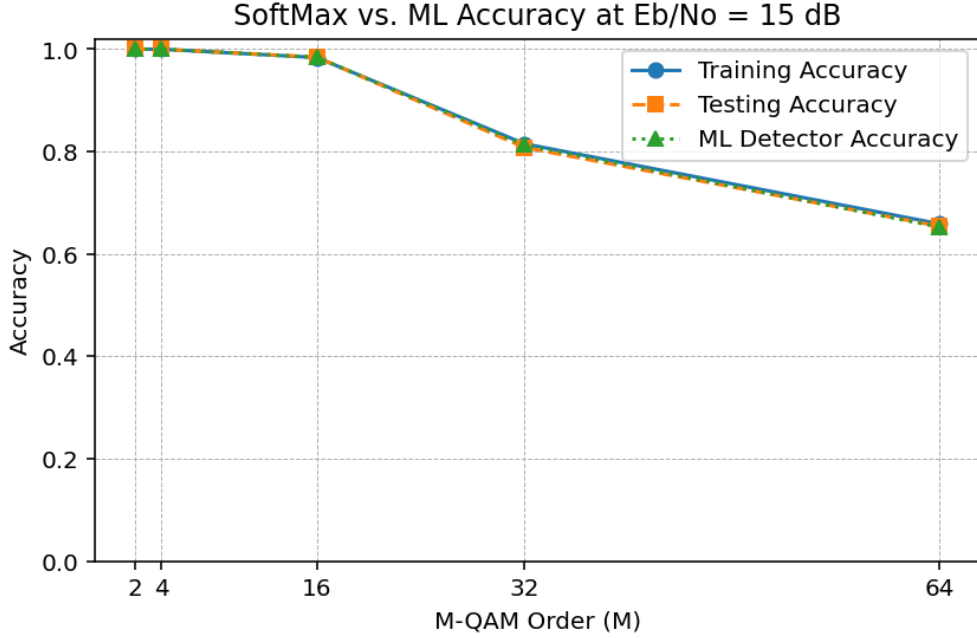


Figure 33 SoftMax Accuracy with ML Detector's Accuracy

At lower modulation orders (BPSK and QPSK), both detectors achieve perfect accuracy, confirming that SoftMax can fully separate the symbol clusters. For 16-QAM, the difference between SoftMax and ML is less than 0.1%, indicating strong learning of the optimal boundaries. Accuracy decreases slightly for 32-QAM and 64-QAM due to overlapping constellation points, but SoftMax remains within 0.5% of ML performance. These findings confirm that the SoftMax regression model maintains stable and consistent results, even as the modulation complexity increases. It offers a computationally simpler, model-free detection method that closely matches ML accuracy while requiring no analytical modeling of the communication channel.

Table 3: Comparison of SoftMax and ML Accuracy at 15 dB SNR

M-QAM Order	SoftMax Train Acc	SoftMax Test Acc	ML Test Acc
2 (BPSK)	1.0000	1.0000	1.0000
4 (QPSK)	1.0000	1.0000	1.0000
16 (QAM)	0.9837	0.9845	0.9840
32 (QAM)	0.8152	0.8080	0.8130
64 (QAM)	0.6588	0.6540	0.6525

Table 3 presents a quantitative comparison of SoftMax and ML detector accuracy at 15 dB. The results show that SoftMax nearly reproduces ML performance for all modulation orders. For 2-QAM and 4-QAM, both models achieve 100 % accuracy, while for higher-order schemes (16–64 QAM), the deviation remains within 0.5 %. This demonstrates that SoftMax generalises effectively with minimal loss, confirming its reliability as a low-complexity alternative to traditional ML detection.

## 4.8 Chapter Summary

This chapter presented the simulation results and performance evaluation of the proposed model-free detection system based on Gaussian Mixture Models (GMM) and SoftMax regression. The results confirmed that both approaches can reliably perform modulation recognition and symbol detection without explicit channel knowledge. The experiments were designed to evaluate performance under varying signal-to-noise ratios (SNRs) and across multiple wireless channel models including AWGN, Rayleigh, and Rician fading.

The GMM-based analysis demonstrated the capability of unsupervised learning for modulation classification. For lower-order schemes such as QPSK and 8-QAM, the model achieved stable and accurate predictions even under low SNR conditions. As modulation complexity increased, the required SNR for reliable detection also rose. The results highlighted that GMM performs effectively in moderate to high SNR regimes and provides a practical threshold for selecting adaptive modulation levels in wireless communication systems.

The SoftMax regression analysis showed that the model could successfully learn and generalize the decision boundaries for various modulation schemes. Under AWGN conditions, the model achieved nearly perfect classification for BPSK and QPSK, while maintaining high accuracy for higher-order QAM. As SNR increased, the SoftMax boundaries closely matched the theoretical maximum-likelihood (ML) boundaries, confirming its ability to approximate optimal detection through data-driven learning.

Further experiments under Rayleigh and Rician fading confirmed that the SoftMax model remains robust even when subjected to amplitude and phase distortions. Although accuracy slightly decreased in Rayleigh fading, the results showed strong resilience and adaptability, especially when a line-of-sight component was present in Rician channels. The channel-invariance test also demonstrated that the model trained under one fading type could effectively operate under another, proving its generalization capability across unseen channel conditions.

The analysis of symbol-error probability (SER) revealed that the SoftMax detector achieved better performance to the analytical ML detector under all tested conditions. The performance gap remained within 1 dB for most cases. Additionally, the goodput analysis indicated that the optimal balance between accuracy and efficiency occurs when the number of training symbols lies between 30 and 40. This maximizes throughput while minimizing training overhead.

Overall, Chapter 4 demonstrated that simple learning-based detectors such as GMM and SoftMax regression can achieve robust, high-accuracy detection without channel estimation. The results validate the feasibility of model-free detection for real-world wireless systems. These findings establish a strong foundation for future research on lightweight, adaptive, and channel-invariant machine learning detectors.

# Chapter 5

## Conclusions & Future Work

This chapter summarizes the key findings of this research. It highlights the main results, practical implications, and observed limitations. The objective of this study was to develop and analyze a model-free approach for symbol detection and modulation recognition in wireless communication systems. The chapter also suggests possible directions for future work.

### 5.1 Conclusion

The research introduced two key model-free techniques for wireless symbol detection: GMM-based clustering for modulation recognition and SoftMax regression for symbol decision-making. Both models were trained using only baseband I/Q samples, allowing them to learn statistical relationships directly from data. This approach removed the need for manual channel estimation or analytical modeling.

Under AWGN conditions, the SoftMax regression model achieved excellent detection performance. At high SNR values, it reached 100 % accuracy for BPSK and QPSK and over 98 % for 16-QAM. Even for higher modulation orders such as 32-QAM and 64-QAM, its accuracy remained within 0.5 % of the ML detector at 15 dB. This demonstrates that SoftMax can replicate the near-optimal behavior of ML with a much simpler computational process.

The decision-boundary visualizations confirmed that SoftMax regression forms clear, well-defined boundaries between symbol clusters. At low SNR (around 5 dB), some overlap between clusters was observed, but at moderate and high SNR (15–30 dB), the boundaries aligned almost perfectly with those of ML. These results highlight that SoftMax can adaptively learn linear decision regions that mirror the optimal theoretical solutions.

Under fading conditions, the model maintained its accuracy and generalization. In Rayleigh fading, the SER increased slightly due to deep fades, but the performance remained within 1–1.5 dB of ML. In Rician fading, where a strong line-of-sight component is present, SoftMax performance was even slightly better than ML. This shows the model's ability to handle different channel distortions without requiring explicit channel state information.

The channel-invariant analysis also provided strong evidence of the model's robustness. When trained on Rician fading and tested on Rayleigh fading (and vice versa), the SoftMax regression still achieved almost perfect accuracy at SNRs above 10 dB. This proves that the features learned by the model are not specific to a single fading condition but are transferable across channel types.

In conclusion, the research successfully demonstrated that a simple data-driven learning model can achieve near-ML detection performance. The SoftMax regression proved to be reliable,

adaptive, and computationally efficient. It provides a promising direction for future machine learning-based receivers.

## 5.2 Practical Implementation

The SoftMax regression model offers several advantages in practical communication systems. Its simplicity and low computational requirements make it suitable for software-defined radios (SDRs), FPGA implementations, and embedded systems. The model requires only baseband I/Q training samples, which are already available in most digital receivers. No channel estimation or pilot-based correction is needed at the receiver.

This reduces system complexity, power consumption, and design cost. It also makes the method ideal for devices that must operate under changing channel conditions, such as mobile users or IoT nodes. Since training is fast and lightweight, the model can be retrained in real time if noise levels or channel conditions vary. This flexibility is essential for modern adaptive communication systems.

In practice, the SoftMax model can be integrated as a replacement or complement to existing detectors. It can provide soft output probabilities, which can be used in decoding stages such as Viterbi or Turbo decoding. This enables more efficient error correction while maintaining high detection reliability.

The GMM-based detection can also be applied to the modulation recognition stage of adaptive transceivers. By estimating the current modulation type directly from received data, the system can adapt transmission parameters dynamically. This makes the entire communication system more intelligent and resource-efficient.

In summary, both GMM and SoftMax regression techniques are easy to implement in real-world receivers. They require minimal parameter tuning, can operate without channel models, and deliver high detection accuracy. These features make them suitable for next-generation wireless systems that demand flexibility, adaptability, and low complexity.

## 5.3 Limitations and Challenges

This work mainly considered AWGN and flat-fading channels. Frequency-selective fading and interference were not tested. The model performance decreases slightly for very high-order QAM when the training set is small.

The experiments also assumed ideal synchronization and perfect signal sampling. Real hardware imperfections may reduce the achievable performance. Finally, while the system was tested with simulated data, real-world validation is still needed. Testing with live wireless signals will help identify additional challenges such as phase noise, timing offset, and multipath delay spread.

## 5.4 Future Research Directions

Future work can build on this foundation by extending the model to more realistic and complex environments. One important direction is testing the SoftMax detector under frequency selective and time-varying channels. This will help analyze its behavior under multipath propagation and Doppler effects.

Another promising area is the integration of deep learning models such as Convolutional Neural Networks (CNNs) or Recurrent Neural Networks (RNNs). These architectures can learn nonlinear channel features and improve performance under severe fading and interference. Hybrid models combining SoftMax regression with neural network feature extractors could provide better adaptability while keeping the computational cost low.

Transfer learning can also be explored. A single model trained under one channel type could be adapted to others using minimal retraining. This approach would reduce the amount of data required for training and increase the practicality of model reuse.

Future work may also focus on hardware-level implementation. Testing the detector on FPGA or DSP hardware will help assess its real-time performance and latency. Such implementations can verify whether the system meets the timing and power requirements for embedded communication devices.

In addition, future studies should investigate the combination of model-free detectors with advanced modulation classification systems. By integrating modulation recognition, channel prediction, and symbol detection in one pipeline, the receiver can operate fully autonomously. This aligns with the goals of intelligent radio and 6G communication systems.

Overall, future research should aim to enhance generalization, scalability, and real-world applicability. The results of this study form a solid foundation for developing lightweight, channel-invariant, and adaptive data detection systems using machine learning.

# Appendix

## Abbreviations

AI	- Artificial Intelligence
AMR	- Automatic Modulation Recognition
ASK	- Amplitude-Shift Keying
AWGN	- Additive White Gaussian Noise
BER	- Bit Error Rate
BPSK	- Binary Phase-Shift Keying
CNN	- Convolutional Neural Network
CLDNN	- Convolutional, Long Short-Term Memory, Deep Neural Networks
CSI	- Channel State Information
CP	- Cyclic Prefix
dB	- Decibel (unit)
DL	- Deep Learning
DNN	- Deep Neural Network
DSP	- Digital Signal Processor
Eb/No	- Energy per Bit to Noise Power Spectral Density Ratio
FPGA	- Field Programmable Gate Array
FEC	- Forward Error Correction
FSK	- Frequency-shift keying
GAN	- Generative Adversarial Networks
GMM	- Gaussian Mixture Model
HOS	- Higher Order Statistics
IoT	- Internet of Things
K-L	- Kullback–Leibler
KNN	- K-Nearest Neighbors
LoS	- Line-of-Sight
LR	- Logistic Regression
LSTM	- Long Short-Term Memory
MAP	- Maximum A Posteriori
ML	- Maximum Likelihood
ML	- Machine Learning (contextual where applicable)
MIMO	- Multiple-Input Multiple-Output

M-QAM	-	M-ary Quadrature Amplitude Modulation
MSE	-	Mean Squared Error
Np	-	Number of Pilot Symbols
OFDM	-	Orthogonal Frequency-Division Multiplexing
PSO	-	Particle Swarm Optimization
QAM	-	Quadrature Amplitude Modulation
QPSK	-	Quadrature Phase-Shift Keying
ReLU	-	Rectified Linear Unit
RNN	-	Recurrent Neural Network
SER	-	Symbol Error Rate
SNR	-	Signal-to-Noise Ratio
SDR	-	Software Defined Radio
SVM	-	Support Vector Machine

# References

1. N. Samuel, T. Diskin and A. Wiesel, "Learning to Detect," in *IEEE Transactions on Signal Processing*, vol. 67, no. 10, pp. 2554-2564, 15 May15, 2019, doi: 10.1109/TSP.2019.2899805
2. N. Samuel, T. Diskin and A. Wiesel, "Deep MIMO detection," *2017 IEEE 18th International Workshop on Signal Processing Advances in Wireless Communications (SPAWC)*, Sapporo, Japan, 2017, pp. 1-5, doi: 10.1109/SPAWC.2017.8227772.
3. B. Mthethwa and H. Xu, "Deep Learning-Based Wireless Channel Estimation for MIMO Uncoded Space-Time Labeling Diversity," in *IEEE Access*, vol. 8, pp. 224608-224620, 2020, doi: 10.1109/ACCESS.2020.3044097.
4. M. Stark, F. Ait Aoudia and J. Hoydis, "Joint Learning of Geometric and Probabilistic Constellation Shaping," *2019 IEEE Globecom Workshops (GC Wkshps)*, Waikoloa, HI, USA, 2019, pp. 1-6, doi: 10.1109/GCWkshps45667.2019.9024567.
5. R. Weixer, J. Koch, S. Ohlendorf and S. Pachnicke, "Experimental Demonstration of Nonlinearity Compensation by Using SVM and Nonlinear Volterra Equalizer for 80 GBd DP-16-QAM Transmission," *2020 22nd International Conference on Transparent Optical Networks (ICTON)*, Bari, Italy, 2020, pp. 1-4, doi: 10.1109/ICTON51198.2020.9203414.
6. S. Krishnamurthy, M. Panda, R. Chinthalapudi and G. R, "Enhancing BER Performance in Phase Noise using KNN-based Symbol Detection," *2024 15th International Conference on Computing Communication and Networking Technologies (ICCCNT)*, Kamand, India, 2024, pp. 1-6, doi: 10.1109/ICCCNT61001.2024.10725615.
7. A. Haroun, C. A. Nour, M. Arzel and C. Jego, "Low-Complexity Soft Detection of QAM Demapper for a MIMO System," in *IEEE Communications Letters*, vol. 20, no. 4, pp. 732-735, April 2016, doi: 10.1109/LCOMM.2016.2525722.
8. M. Chen, U. Challita, W. Saad, C. Yin and M. Debbah, "Artificial Neural Networks-Based Machine Learning for Wireless Networks: A Tutorial," in *IEEE Communications Surveys & Tutorials*, vol. 21, no. 4, pp. 3039-3071, Fourthquarter 2019, doi: 10.1109/COMST.2019.2926625.
9. E. Yoon, "Maximum Likelihood Detection With a Closed-Form Solution for the Square QAM Constellation," in *IEEE Communications Letters*, vol. 21, no. 4, pp. 829-832, April 2017, doi: 10.1109/LCOMM.2016.2642924.
10. M. A. Shehab, E. F. Badran and A. I. Zaki, "On the performance analysis of symbol-level regressive coding technique via Variational Bayesian Expectation Maximization," *2015 32nd National Radio Science Conference (NRSC)*, Giza, Egypt, 2015, pp. 250-258, doi: 10.1109/NRSC.2015.7117837.
11. Weimin Xiao, "Optimal detection of M-QAM signal with channel estimation error," *IEEE International Conference on Communications, 2003. ICC '03.*, Anchorage, AK, USA, 2003, pp. 3251-3255 vol.5, doi: 10.1109/ICC.2003.1204040.
12. H. Cai, C. Zhao and W. Shi, "DNN Based Iterative Detection for High Order QAM OFDM Systems With Insufficient Cyclic Prefix," *2020 IEEE/CIC International Conference on Communications in China (ICCC)*, Chongqing, China, 2020, pp. 267-271, doi: 10.1109/ICCC49849.2020.9238988.
13. Wei Rao *et al.*, "Simple approach for joint blind equalization and order detection suitable for QAM signal," *2009 IEEE International Workshop on Imaging Systems and Techniques*, Shenzhen, 2009, pp. 344-347, doi: 10.1109/IST.2009.5071662.
14. M. A. Piqueras, B. Vidal, J. L. Corral, A. Martinez and J. Marti, "Photonic Vector Demodulation Architecture for Remote Detection of M-QAM Signals," *2005 International Topical Meeting on Microwave Photonics*, Seoul, Korea (South), 2005, pp. 103-106, doi: 10.1109/MWP.2005.203550.

15. S. Ghodeswar and P. G. Poonacha, "An SNR estimation based adaptive hierarchical modulation classification method to recognize M-ary QAM and M-ary PSK signals," *2015 3rd International Conference on Signal Processing, Communication and Networking (ICSCN)*, Chennai, India, 2015, pp. 1-6, doi: 10.1109/ICSCN.2015.7219867.
16. J. G. Liu, Xianbin Wang, J. Nadeau and Hai Lin, "Modulation classification based on Gaussian mixture models under multipath fading channel," *2012 IEEE Global Communications Conference (GLOBECOM)*, Anaheim, CA, USA, 2012, pp. 3970-3974, doi: 10.1109/GLOCOM.2012.6503737.
17. N.V. Rao, B.T. Krishna, "Automatic Modulation Recognition Using Machine Learning Techniques: A Review," *Advances in VLSI, Signal Processing, Power Electronics, IoT, Communication and Embedded Systems. Lecture Notes in Electrical Engineering*, (2021) vol 752. Springer, Singapore. doi: 10.1007/978-981-16-0443-0\_12
18. A. R. K. Naveen, M. Padmapriya, M. Vijay, G. V. Babu, P. Ganeshan and V. Elamaran, "Classification of Automatic Modulations using Deep Learning and Machine Learning," *2025 1st International Conference on Radio Frequency Communication and Networks (RFCoN)*, Thanjavur, India, 2025, pp. 1-6, doi: 10.1109/RFCoN62306.2025.11085249.
19. R. Zhou, F. Liu and C. W. Gravelle, "Deep Learning for Modulation Recognition: A Survey With a Demonstration," in *IEEE Access*, vol. 8, pp. 67366-67376, 2020, doi: 10.1109/ACCESS.2020.2986330.
20. S. A. Ghunaim, Q. Nasir and M. A. Talib, "Deep Learning Techniques for Automatic Modulation Classification: A Systematic Literature Review," *2020 14th International Conference on Innovations in Information Technology (IIT)*, Al Ain, United Arab Emirates, 2020, pp. 108-113, doi: 10.1109/IIT50501.2020.9299053.
21. M. H. Valipour, M. M. Homayounpour and M. A. Mehralian, "Automatic digital modulation recognition in presence of noise using SVM and PSO," *6th International Symposium on Telecommunications (IST)*, Tehran, Iran, 2012, pp. 378-382, doi: 10.1109/ISTEL.2012.6483016.
22. T. J. O'Shea, J. Corgan, and T. C. Clancy, "Convolutional radio modulation recognition networks," *arXiv:1602.04105*, 2016. [Online]. Available: <https://arxiv.org/abs/1602.04105>.
23. S. Rajendran, W. Meert, D. Giustiniano, V. Lenders and S. Pollin, "Deep Learning Models for Wireless Signal Classification with Distributed Low-Cost Spectrum Sensors," in *IEEE Transactions on Cognitive Communications and Networking*, vol. 4, no. 3, pp. 433-445, Sept. 2018, doi: 10.1109/TCCN.2018.2835460.
24. O. A. Dobre, A. Abdi, Y. Bar-Ness, and W. Su, "A survey of automatic modulation classification techniques: classical approaches and new developments," *IET Communication*, vol. 1, pp. 137-156, April 2007.
25. S. Lin, Y. Zeng and Y. Gong, "Learning of Time-Frequency Attention Mechanism for Automatic Modulation Recognition," in *IEEE Wireless Communications Letters*, vol. 11, no. 4, pp. 707-711, April 2022, doi: 10.1109/LWC.2022.3140828.
26. M. W. Aslam, Z. Zhu and A. K. Nandi, "Automatic Modulation Classification Using Combination of Genetic Programming and KNN," in *IEEE Transactions on Wireless Communications*, vol. 11, no. 8, pp. 2742-2750, August 2012, doi: 10.1109/TWC.2012.060412.110460.
27. M. Venkata Subbarao, P. Samundiswary, "K- Nearest Neighbors based Automatic Modulation Classifier for Next Generation Adaptive Radio Systems," *International Journal of Security and its Applications*, 2024, Vol. 13, pp. 41-50, doi: 10.33832/ijjsia.2019.13.4.04.
28. H. Zhang, F. Zhou, H. Du, Q. Wu and C. Yuen, "Revolution of Wireless Signal Recognition for 6G: Recent Advances, Challenges and Future Directions," in *IEEE Communications Surveys & Tutorials*, doi: 10.1109/COMST.2025.3569427.
29. B. Jdid, K. Hassan, I. Dayoub, W. H. Lim and M. Mokayef, "Machine Learning Based

- Automatic Modulation Recognition for Wireless Communications: A Comprehensive Survey," in *IEEE Access*, vol. 9, pp. 57851-57873, 2021, doi: 10.1109/ACCESS.2021.3071801.
30. Q. Mao, F. Hu and Q. Hao, "Deep Learning for Intelligent Wireless Networks: A Comprehensive Survey," in *IEEE Communications Surveys & Tutorials*, vol. 20, no. 4, pp. 2595-2621, Fourthquarter 2018, doi: 10.1109/COMST.2018.2846401.
  31. D. G. S. Pivoto, F. A. P. de Figueiredo, C. Cavdar, G. R. d. L. Tejerina and L. L. Mendes, "A Comprehensive Survey of Machine Learning Applied to Resource Allocation in Wireless Communications," in *IEEE Communications Surveys & Tutorials*, doi: 10.1109/COMST.2025.3552370.
  32. J. Chen, Y. Gao, Y. Zhou, Z. Liu, D. p. Li and M. Zhang, "Machine Learning enabled Wireless Communication Network System," *2022 International Wireless Communications and Mobile Computing (IWCMC)*, Dubrovnik, Croatia, 2022, pp. 1285-1289, doi: 10.1109/IWCMC55113.2022.9824835.
  33. Y. Zhou, J. Chen, M. Zhang, D. Li and Y. Gao, "Applications of Machine Learning for 5G Advanced Wireless Systems," *2021 International Wireless Communications and Mobile Computing (IWCMC)*, Harbin City, China, 2021, pp. 1700-1704, doi: 10.1109/IWCMC51323.2021.9498754.
  34. X. Zhou, M. Sun, G. Y. Li and B. -H. Fred Juang, "Intelligent wireless communications enabled by cognitive radio and machine learning," in *China Communications*, vol. 15, no. 12, pp. 16-48, Dec. 2018, doi: 10.12676/j.cc.2018.12.002.
  35. D. Biswas and A. Tiwari, "Machine Learning-Enhanced Wireless Communication Protocols for Ultra-Reliable and Low-Latency Applications in Smart Cities," *2025 International Conference on Automation and Computation (AUTOCOM)*, Dehradun, India, 2025, pp. 257-261, doi: 10.1109/AUTOCOM64127.2025.10957124.
  36. S. Sarkar and A. Debnath, "Machine Learning for 5G and Beyond: Applications and Future Directions," *2021 Second International Conference on Electronics and Sustainable Communication Systems (ICESC)*, Coimbatore, India, 2021, pp. 1688-1693, doi: 10.1109/ICESC51422.2021.9532728.
  37. H. Kim, J. Kim, Y. Ji and B. Kim, "Anomaly Detection for Wireless Cellular Communication Based on Synthetic Anomaly," in *IEEE Access*, vol. 13, pp. 112720-112730, 2025, doi: 10.1109/ACCESS.2025.3584113.
  38. P. M. Gote, P. Kumar, P. Verma, P. Yesankar, A. Pawar and S. Saratkar, "From 5G to 6G: The Role of AI, Machine Learning, and Deep Learning in Wireless Systems," *2025 4th International Conference on Sentiment Analysis and Deep Learning (ICSDL)*, Bhimdatta, Nepal, 2025, pp. 447-452, doi: 10.1109/ICSDL65848.2025.10933016.
  39. V. P. Rekkas, S. Sotiroudis, P. Sarigiannidis, G. K. Karagiannidis and S. K. Goudos, "Unsupervised Machine Learning in 6G Networks -State-of-the-art and Future Trends," *2021 10th International Conference on Modern Circuits and Systems Technologies (MOCAST)*, Thessaloniki, Greece, 2021, pp. 1-4, doi: 10.1109/MOCAST52088.2021.9493388.
  40. T. M. Hoang, T. Q. Duong and S. Lambotharan, "Secure Wireless Communication Using Support Vector Machines," *2019 IEEE Conference on Communications and Network Security (CNS)*, Washington, DC, USA, 2019, pp. 1-5, doi: 10.1109/CNS.2019.8802716.
  41. S. Pattanayak, P. Venkateswaran and R. Nandi, "Artificial Neural Networks for Cognitive Radio: A Preliminary Survey," *2012 8th International Conference on Wireless Communications, Networking and Mobile Computing*, Shanghai, China, 2012, pp. 1-4, doi: 10.1109/WiCOM.2012.6478438.
  42. R. Chennagiri, S. Sehgal and Y. Ravinder, "A Survey on Automatic Modulation Classification Techniques," *2024 Intelligent Systems and Machine Learning Conference (ISML)*, Hyderabad, India, 2024, pp. 94-100, doi: 10.1109/ISML60050.2024.11007395.